1 Introduction

1.1 The branched chain aminotransferase proteins

Like all key aminotransferase enzymes, there are two predominant isoforms of the human branched chain aminotransferase (hBCAT) enzyme [E.C. 2.6.1.42]; cytosolic hBCAT (hBCATc) and mitochondrial hBCAT (hBCATm). These hBCAT proteins share 58% homology in their primary amino acid sequence and share 29% homology with the corresponding enzyme in e-coli (Davoodi *et al.,* 1998; Hutson *et al.*, 1988; Hutson *et al.*, 1992). The BCAT1 (hBCATc) gene is a c-myc regulated gene and maps to the human 12p12 chromosome, whereas the BCAT2 (hBCATm) gene is a Klf-15 regulated gene (at least partially) and maps to the human 19q13 chromosome (Ben-Yosef *et al.*, 1998; Benvenisty *et al.*, 1992; Kuo *et al*., 2013). Both genes are located close to Ras genes so are likely to be the result of an evolutionary duplication event involving both the Ras and BCAT genes (Ben-Yosef *et al*., 1998).

The other key aminotransferases are alanine aminotransferase [E.C. 2.6.1.2] and aspartate aminotransferase [E.C. 2.6.1.1]. All are pyridoxal phosphate (PLP, vitamin-B_6) dependent and have both cytosolic and mitochondrial isoforms. Based on the three dimensional structures of these aminotransferases they have been separated into four family subtypes (Jansonius, 1998; Mehta & Christen, 2000; Salzmann *et al.*, 2000; Schneider *et al.*, 2000). Most of the PLP dependent aminotransferases belong to the fold type I family. The hBCAT enzymes belong to the fold type IV aminotransferase family, and are the only mammalian enzymes in this family (Yennawar *et al.,* 2001; Yennawar *et al.,* 2002). The hBCAT protein is in the fold type IV

aminotransferase family due to the fact that the cofactor PLP is located at the bottom of the active site with the re-face toward the protein side forming a covalent Schiff base with the side chain of the catalytic lysine group (Yoshimura *et al.*, 1996).

1.2 The transamination and oxidation of the BCAAs

The function of the hBCAT proteins is to catalyse the reversible transamination of the branched chain amino acids (BCAAs) leucine, isoleucine and valine to their respective ketoacids; α-ketoisocaproate (KIC), α-ketoisovalerate (KIV) and α-keto-β-methylvalerate (KMV) and glutamate (Figure 1.1) (Ichihara & Koyama, 1966). The BCAT enzymes are specific to BCAAs with substrate preferences of isoleucine ≥ leucine > valine >> glutamate (Hall, 1993; Wallin, 1990). Non-substrate amino acids, such as the aromatic amino acids (phenyalanine, tryptophan, tyrosine and histidine), are either unable to interact through van der Waals interactions or have steric clashes within the active site (Conway *et al*., 2003). For the deamination of the BCAAs and the reamination of the branched chain α-keto acids (BCKAs) the k_{cat} and K_m imply the hBCATc reaction (Kcat/Km of $220x10^3 m^{-1}s^{-1}$ for leucine) is between 2 and 5 times faster than for hBCATm (Kcat/Km of 88 $x10^3 m^{-1}s^{-1}$ for leucine) (Table 1.1) (Davoodi *et al*., 1998). As the active site residues demonstrate similar cofactor binding it was proposed that the residues around the active site were responsible for these kinetic differences (Hall *et al*., 1993).

The kinetics of both hBCAT enzymes follows a 'Ping-Pong' reaction (Christen *et al*., 1985; Hall *et al*., 1993; Kiick & Cook, 1983). The α-carbon atom of the carboxyl group forms an electrostatic interaction with a positively charged amino

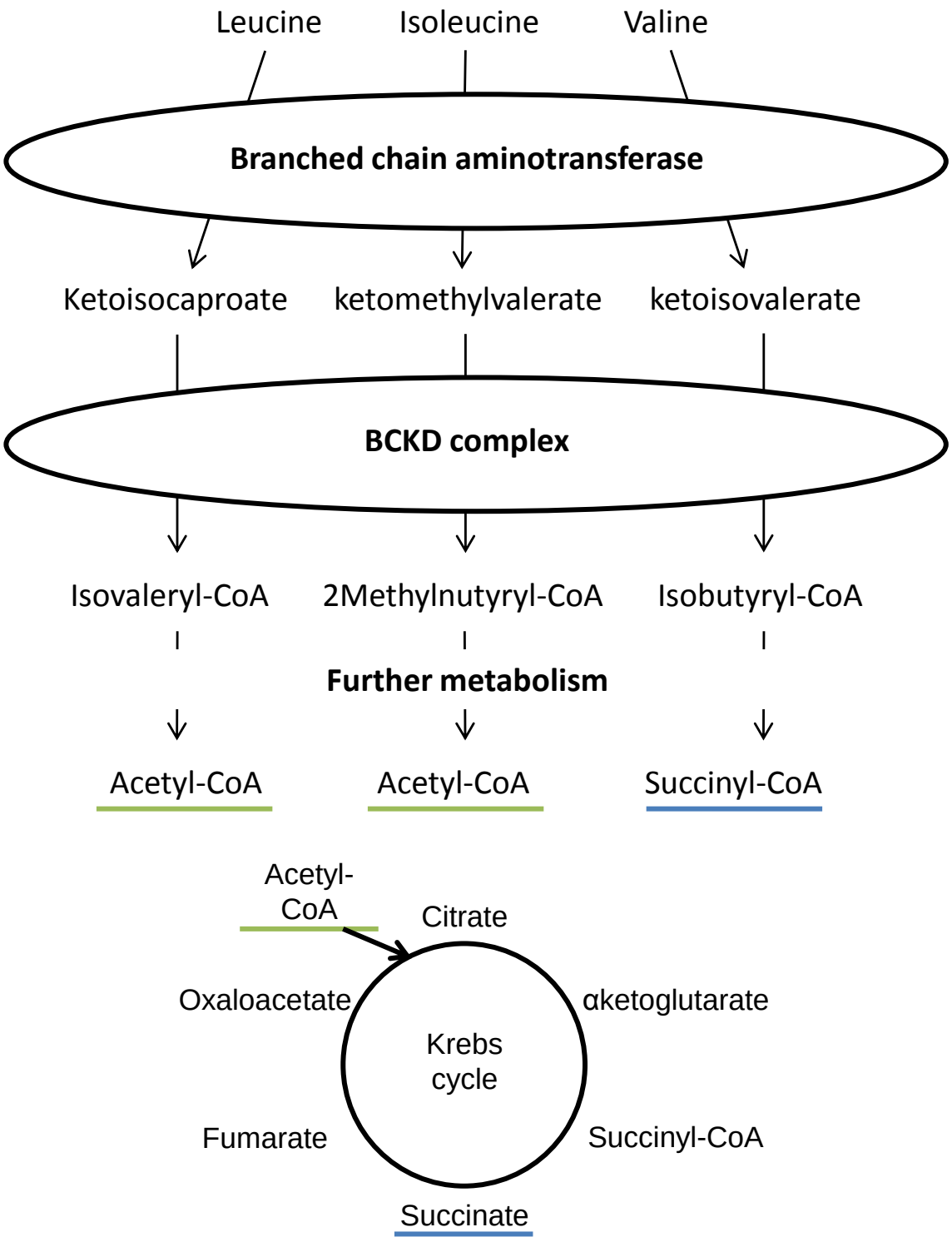

Figure 1. 1 The metabolism of the branched chain amino acids. The first step shows the transamination of the branched chain amino acids into their respective keto acids. These are then further metabolised by the BCKD complex into the CoA products. These can then be further metabolised into Krebs cycle intermediates such as Acetyl-CoA (in the case of leucine and isoleucine), or succinyl-CoA (in the case of isoleucine and valine) (adapted from Hutson *et al*., 2005). Abbreviations: BCKD – branched chain keto acid dehydrogenase complex.

Substrate	hBCATm K_{cat}	hBCATm K_m	hBCATm K_{cat}/K_m	hBCATc K_{cat}	hBCATc K_m	hBCATc K_{cat}/K_m
BCAA	s^{-1}	mM	$x10^3M^{-1}s^{-1}$	s^{-1}	mM	$x10^3M^{-1}s^{-1}$
Leu	106 ± 11	1.21 ± 0.12	88	132 ± 7	0.60 ± 0.04	220
Ile	80 ± 1	0.60 ± 0.02	165	172 ± 9	0.77 ± 0.02	223
Val	68 ± 2	6.1 ± 0.11	11	122 ± 8	2.40 ± 0.09	51

Table 1. 1 Kinetic constants of the hBCAT proteins Kinetic constants of the hBCAT proteins. K_m and K_{cat} values were obtained from hyperbolic plots fit to the Michaelis-Menten equation. Activity of the hBCATm protein is between 2-5 times less than that of the hBCATc protein (Davoodi *et al*., 1998).

acid residue within the active site of the enzyme. The α-hydrogen atom of the substrate amino acid (BCAAs) forms a Schiff-base with PLP which is subsequently removed (with the amine group) by the catalytic base of the enzyme and transferred to the C4 of PLP to produce a pyridoxamine (PMP) intermediate form of the enzyme, and releases the respective BCKA (first half reaction). The PMP-enzyme subsequently aminates α-ketoglutarate (α-KG) to produce glutamate and restore the PLP form of the enzyme (second half reaction) (Figure 1.2).

The second step in this metabolic pathway, which is considered the rate limiting step, is the irreversible oxidative decarboxylation of the BKCAs catalysed by the mitochondrial BKCA dehydrogenase enzyme complex (BCKD) forming the branched chain acyl Co-A derivatives (Harris, 1986; Hutson *et al*., 2005) (Figure 1.1). The BCKD complex is organised into a 24-meric unit consisting of dihydrolipoamide acyltransferase (E2) to which multiple BCKA dehydrogenases (E1) and dihydrolipoamide dehydrogenase (E3) non-covalently bind (Petti *et al.*, 1978). The E1 subunit catalyses the thiamine diphosphate decarboxylation of the BCKAs to produce carbanion-thiamine diphosphate (Damuni *et al.*, 1985). This is subsequently transferred to the E2 subunit by the carbanion to the lipoyl moiety, with the acyl group transferred to the E2 active site (Brautigam *et al.*, 2006). The dihydrolipoyl residue is re-oxidized by the FAD moiety of E3, where NAD^+ is the electron acceptor. The E1 subunit also has the capacity to weakly associate with hBCATm (likely through the CXXC motif) with a K_D of 2.8 μM and is proposed to channel BKCAs to the BCKD complex (Islam *et al*., 2007; Islam *et al*., 2010). The BCKD complex is regulated through phosphorylation, with the phosphorylated protein having decreased activity. It is also apparent that the

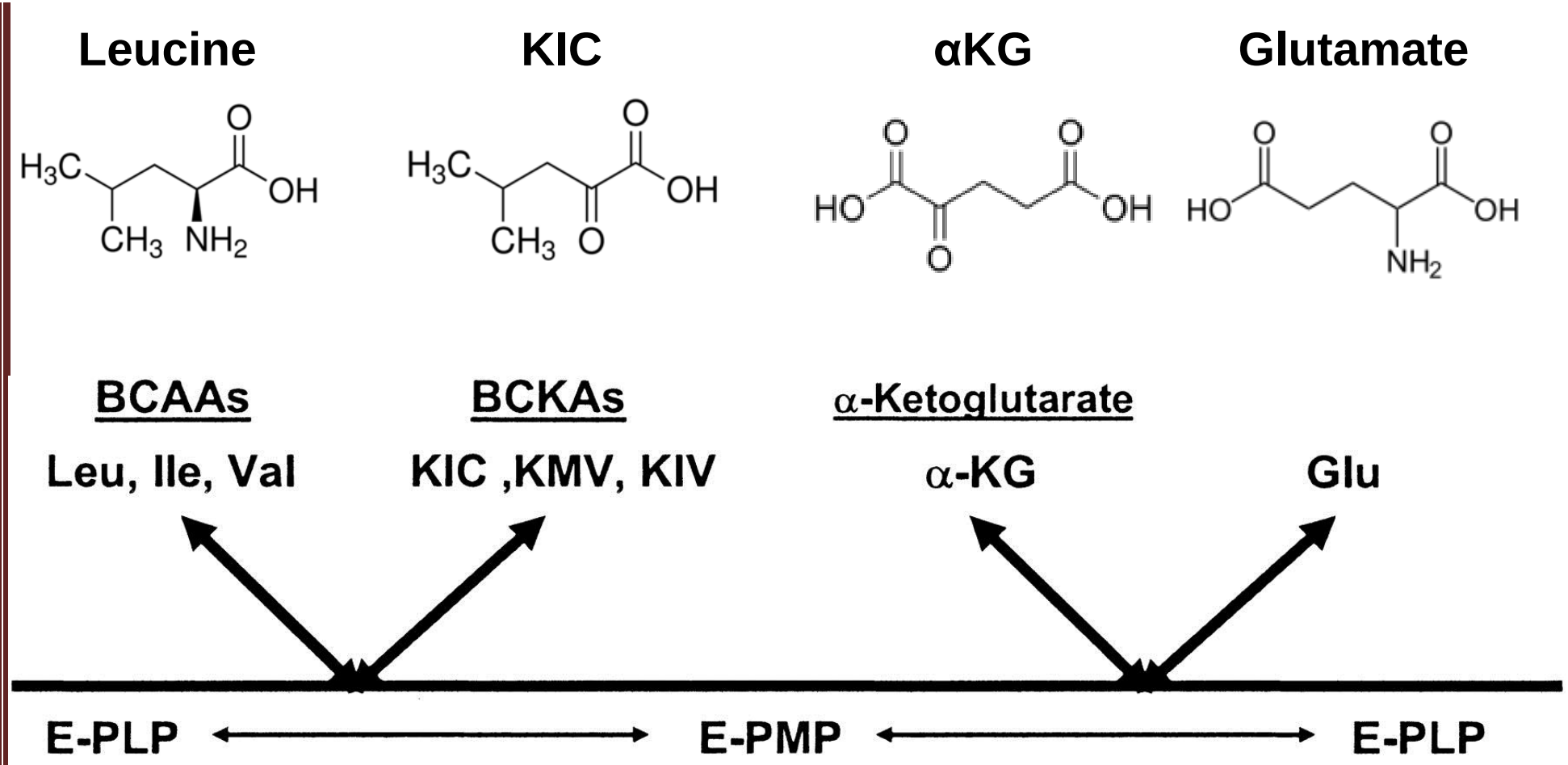

Figure 1. 2 Ping-Pong kinetics of the hBCAT protein. First, the PLP bound form of hBCAT (E-PLP) transfers the amino group from the BCAA, resulting in the BCKA, to the PLP – forming the PMP form of the hBCAT proteins (E-PMP). α-ketoglutarate (α-KG) can only bind to the E-PMP form, which has the amino group transferred to it, forming glutamate and regenerating the E-PLP form (Hutson *et al.,* 2005; Islam *et al.*, 2010).

binding of hBCATm is also regulated through phosphorylation, as phosphorylated E1 is unable to associate with hBCATm (Islam *et al.*, 2007).

Recently glutamate dehydrogenase (GDH1) has also been identified as a binding partner of BCATm as observed in rat tissue (Hutson *et al.*, 2011; Islam *et al.*, 2010). It was demonstrated that GDH1 binds to the PMP form of BCATm but not to the PLP form. This protein interaction facilitates re-amination of α-KG by GDH1 oxidative deamination reaction. This interaction between GDH1 and BCATm promotes the regeneration of PLP-BCATm, which is proposed to subsequently bind to the BCKD complex promoting the net nitrogen transfer from the BCAAs. This will also lead to the production of free ammonia that has been demonstrated to be important for astrocyte glutamine synthesis in the central nervous system of rodents (Hutson *et al.*, 2011; Islam *et al.*, 2010).

1.3 3D structure for hBCATm and hBCATc

Initial purification of the BCAT protein was performed in 1965 by Ichihara *et al.,* (Ichihara *et al.*, 1965; Taylor & Jenkins, 1966) and much of the initial work on the BCAT protein was predominantly utilising on hog heart and rats (Taylor *et al*., 1970; Ogawa *et al*., 1972). This work demonstrated that protein activity required a reducing environment (i.e. the presence of β-mercaptoethanol), with a pH optimum of 8.3 (Taylor *et al*., 1970). Bacteria contain a single BCAT isoform, compared to mammals which generally have two (although mice have another aminotransferase specific to leucine localised to the liver) (Ikeda *et al*., 1976).

Utilising molecular replacement methods and crystal structures (with ketamine, PMP and TRIS) the structure of hBCATm has been revealed as a homodimer, two monomers linked by an interdomain loop 11 amino acids in length, with the active site located close to the dimer interface. Each monomer is 365 amino acids in length and is composed of a small domain (1-175) and a large domain (176-365). Each domain contains four α-helical structures with the small subunit containing an additional funnel twisted β-pleated sheet and the large domain also containing ten-stranded β-pleated sheets. The 4'-aldehyde group of PLP covalently binds to the ε-amino group of the active site Lys202 (Figure 1.3). Tyr207 and Glu237 anchor the PLP securely at the bottom of the active site cavity and Thr313, Arg99, Val269 and Val270 form strong hydrogen bonds with the phosphate oxygen together with two water molecules. The key residues in the substrate binding pocket are Phe75, Tyr207, Thr240 (surface A) Phe30, Tyr141, Ala314 (surface B), Tyr70*, Leu153* and Val155* (Surface C) (*from the opposite subunit). It was noted that these residues were predominantly hydrophobic, relating to the hydrophobic nature of the BCAAs. Domain closure is governed by residue Tyr173 (essential for catalysis), a part of the interdomain loop that can adopt various conformations to aid active site access or exit of substrates and products. This Tyr173 also forms a weak hydrogen bond interaction with Cys315, however under oxidizing conditions this is disrupted causing the reorientation of Tyr173 away from the active site. Key residues Phe30, Arg143, Tyr207 and Arg141 are also re-orientated decreasing substrate side chain binding.

For hBCATc the crystal structure was finally resolved by Goto *et al.*, (2008) complexed with gabapentin and 4-methyvalerate. Although larger than

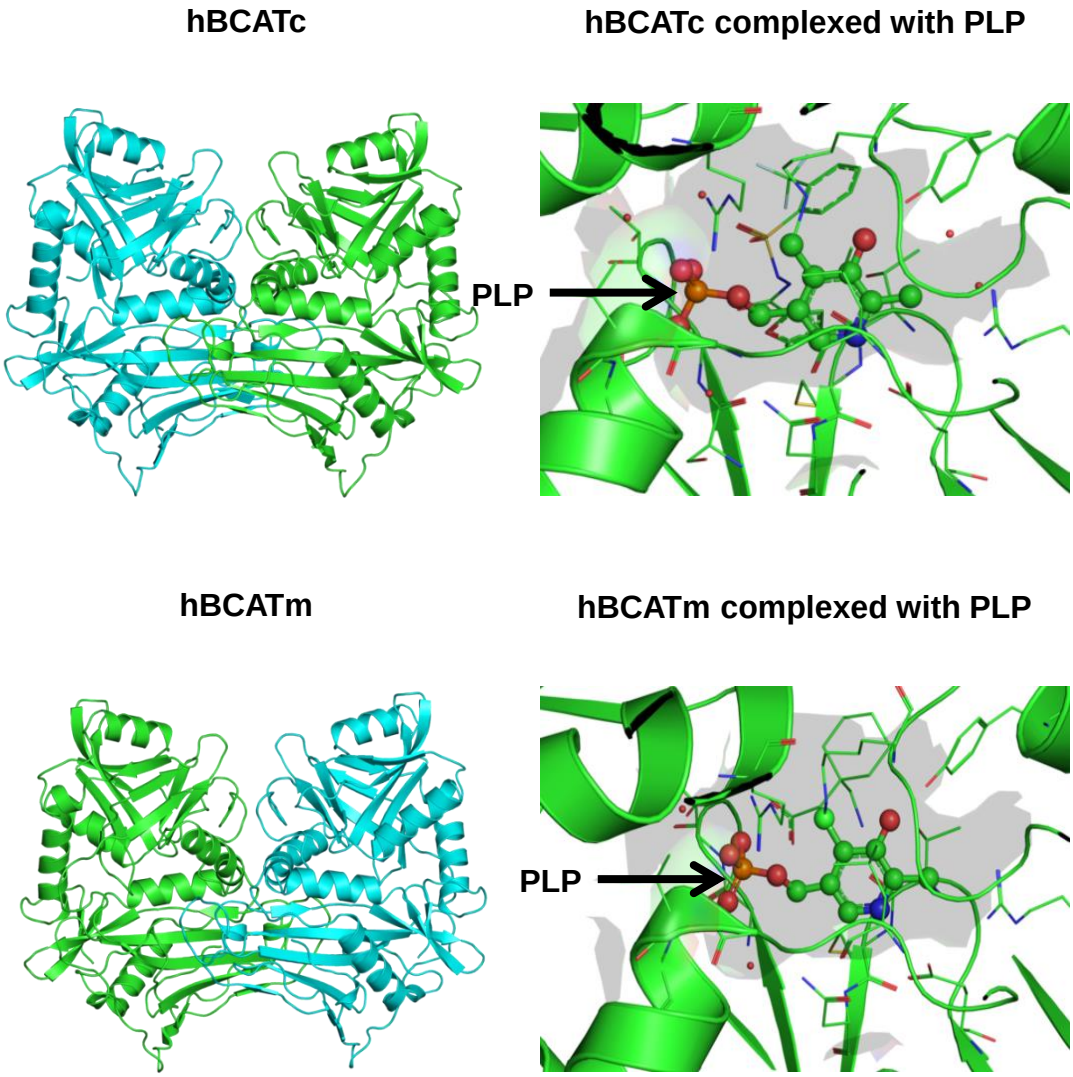

Figure 1. 3 Complete structure of the hBCATc and hBCATm protein with complexed PLP. Both hBCATc and hBCATm are homodimers in the active state with the active site requiring residues from the opposite monomer. Each monomer has a large and a small domain. Structures are also largely quite similar as is the PLP binding pocket. The PLP binds with its re-face directed towards the protein forming a Schiff base with a Lys residue (Lys222 for hBCATc, Lys202 for hBCATm) (acquired from the European Bioinformatics Institute).

hBCATm, at 395 amino acids, each monomeric form of hBCATc also consists of a small domain (1-188), an interdomain loop (189-201) and a large domain (202-395). Both the small and large domain are folded into an open α/β pseudo-barrel structure with PLP having similar alignment to that in hBCATm (Lys222) (Figure 1.3). The substrate binding pocket for hBCATc is identical to that for hBCATm with the exception of one residue (Val336 in hBCATc for Gln336 in hBCATm). Also observed is that hBCATc (similar to that of hBCATm) contains a tyrosine residue (Tyr193) of the interdomain loop that dictates the access of substrates to the active sites. The main groups that enclose the gabapentin structure include Tyr90*, Arg163, Tyr161, Gly97 and two water molecules.

1.4 Unique redox-active CXXC of the hBCAT proteins

Another unique aspect of mammalian BCAT in comparison to bacterial BCAT is the presence of a reactive CXXC motif (Cys315-Gln336-Val337-Cys318 for hBCATm, Cys335-Val336-Val337-Cys338 for hBCATc) that is located 10 Å from the active site (Conway *et al.*, 2002; Conway *et al.*, 2003). The CXXC motif, through a network of hydrogen bonds, plays a crucial role in orientating the substrate optimally for catalysis. Disordering of the N-terminal loop occurs through oxidation of the CXXC motif and this disrupts the integrity of the N-terminal binding pocket, particularly for the branched chain side chains (Yennawar *et al*., 2006). This oxidation predominantly effects the second half reaction rather than the first with the disruption of the CXXC motif resulting in altered substrate orientation and an unprotonated PMP amino group rendering the enzyme catalytically inactive (Yennawar *et al*., 2006).

Site-directed mutagenesis identified the N-terminal cysteine as the 'redox sensor' and the C-terminal cysteine as the resolving partner (Conway *et al.*, 2004). Under oxidizing conditions these cysteine residues form disulphide bonds through the production of a sulphenic acid intermediate acting as a 'redox switch', reducing enzyme activity, protecting the protein active site and protecting the sulphur groups from irreversible sulphur based adduct formation (Figure 1.4) (Conway *et al.*, 2002; Conway *et al.*, 2004). Hydrogen peroxide induces complete (reversible) inactivation of hBCATm, whereas air oxidation alone results in an ~40% loss of hBCATc activity with no further loss observed on hydrogen peroxide treatment (Conway *et al*., 2008). Low concentrations of GSNO cause a time dependent loss of hBCAT activity with hBCATc less sensitive to GSNO than hBCATm (50% and 77% loss of activity respectively). This loss of activity is associated with increased S-glutathionylation and partial dimerisation for hBCATc, with the loss of activity not fully appreciated for hBCATm but possibly caused by a loss of dimerisation (catalytically competent hBCAT is a dimer) (Coles *et al.*, 2009; Davoodi *et al.*, 1998; Yennawar *et al*., 2001). This CXXC disulphide bond is reversible by isomerase proteins, an example of which is protein disulphide isomerase (PDI) (Figure 1.4).

The PDI protein is a 55-kDa protein containing four thioredoxin domains (*a-b-b'-a'*) with the two *a* domains containing the active CXXC motifs (CGHC). The protein is 508 amino acids in length with an interdomain region of 19 residues connecting the *b'* to the *a'* domain (Freedman *et al*., 1998). It is referred to as a thiol-disulphide oxidoreductase and is predominantly restricted to the endoplasmic reticulum (ER) by an ER retrieval motif (KDEL) (Pelham, 1990). The 'b' domains have no reactive cysteines and are instead made up of more

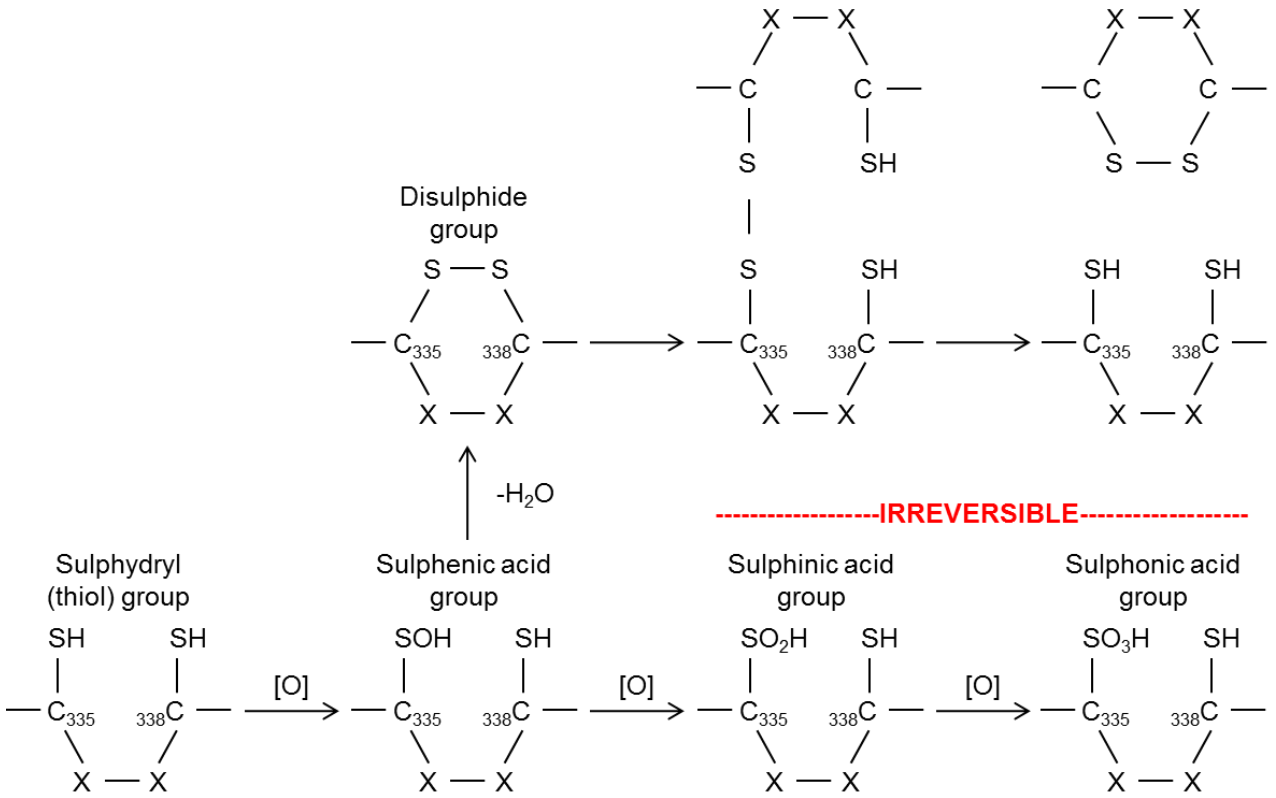

Figure 1. 4 Oxidation of the thiol group and reversal of the disulphide formation in the hBCATc protein. Inactivation occurs after an oxidizing event of the thiol group, followed by disulphide bond formation. This is reversed in the case of the disulphide bond group and sulphenic acid group by a reducing event such as glutathione or glutaredoxin. The sulphinic and sulphonic acid groups are generally irreversible (particularly sulphonic groups) in nature but may provide an 'emergency' signalling role with regards to cell redox status. Sulphinic and sulphonic acid groups are unlikely to form on hBCATc or hBCATm CXXC sulphur groups due to the speed at which disulphide formation occurs, these adducts are more common in non-disulphide bond forming reactive cysteines. The CXXC motif reversing the disulphide bond formation may be from redox associated enzymes such as glutaredoxin or protein disulphide isomerase. The disulphide bond formed on this protein (glutaredoxin of protein disulphide isomerase) is reversed by the addition of 2 GSH molecules that restore the CXXC motif and produce GSSG that can go to produce more GSH via glutathione reductase (Conway, et al. 2004; Dalle-Donne et al., 2007; Herrero & Torre-Ruiz, 2007; Poole & Nelson, 2008).

hydrophobic residues responsible for substrate recognition, orientation and binding (Freedman *et al*., 1998). The PDI protein carries out thiol oxidation or reduction to correct disulphides in proteins via its CXXC motifs, but PDI also has chaperone activities that are not related to the CXXC motif and thought to act as a prelude to correct folding (Hatahet & Ruddock, 2009; Imaoka, 2011). The rates of PDI catalysed reactions are most dependent on the substrate and the S-glutathione (GSH) to glutathione disulphide (GSSG) ratio (Hatahet & Ruddock, 2009).

There are over 20 proteins in the PDI family and there have been two other variants described that are homologous to hBCATm: a novel alternatively spliced variant localised in placental tissue and a splice variant that acts as a co-repressor of thyroid hormone nuclear receptors (Than *et al.,* 2001; Lin *et al.,* 2001). This inhibition of thyroid hormone nuclear receptor is proposed to be mediated by histone deacetylase activity of the hBCATm variant (Lin *et al*., 2001).

1.5 Distribution of the BCAT proteins in mammalian models.

Due to the importance of the hBCAT proteins in metabolising the essential BCAAs their location in animal and cell models have been extensively studied (Bonfils *et al.*, 2000; Bixel *et al.*, 1997; Bixel *et al.*, 2001; Garcia-Espinosa *et al.*, 2007; Sweatt *et al.*, 2004[a,b]). In cell culture systems Bixel *et al.,* (1997 & 2000) observed BCATc localised in neurons and developing oligodendrocytes, whereas the BCATm isoform was localised predominantly in astroglia. It was also evident that BCATm and BCATc expression did not co-localise within the same cell type, probably due to a form of biochemical redundancy.

Further work to that performed in culture has commonly been in mice, rats, pigs or sheep (Bonfils *et al*., 2000; Faure *et al*., 1999; Torres *et al*., 1998). Work in sheep localised BCATc expression to skeletal muscle, which is the predominant site of BCAA transamination in these animals (Bonfils *et al*., 2000). Other work has localised BCATm to sheep placenta (Faure *et al*., 1999). The work in sheep differs somewhat to that of other mammals in that the mitochondrial isoform contributes to 57-71% of BCAT activity in sheep skeletal muscle whereas BCATc was at barely detectable levels in other mammalian skeletal muscle (Faure *et al*., 1999). This was attributed to the differences in metabolism of ruminants (sheep) from omnivores (mice, rats and humans) (Bonfils *et al*., 2000).

Contrary to work on ruminants, Hutson (1988) demonstrated that muscle BCAT activity in rats was predominantly mitochondrial in nature with cytosolic activity only present in muscles with a high white fibre composition. In these studies, rat BCATm activity was highest in heart tissue, followed by skeletal muscle, kidney cortex and a small presence in the brain with the majority of brain BCAT activity cytosolic in nature. There was no BCAT activity in the liver (Hutson *et al*., 1988; Hutson, 1988). In rats, the mRNA levels of BCATm are highest in the stomach, followed by the kidney, heart, muscle, brain, skin and lung. No BCATm mRNA was detectable in the liver (Torres *et al*., 1998). Mice BCATc has the highest activity within the testis and heart (Montamat *et al*., 1978).

Sweatt *et al.,* (2003) further investigated the hBCAT distribution and demonstrated that hBCATm was distributed throughout the digestive tract,

pancreas, uterus, testis, stomach and the transporting epithelium of the convoluted tubules in the kidney. It was further noted that hBCATm expression was intense in secretory cells. The mitochondrial isoform, hBCATm plays a significant role in skeletal muscle glutamine and alanine synthesis (Suryawan *et al.*, 1998; Yennawar *et al*., 2001; Yoshizawa, 2004). Expression of hBCATc was localised in cells of the autonomic innervation of the digestive tract and the axons of the sciatic nerve (Sweatt *et al*., 2003). In human skeletal muscle hBCATm activity is higher than that of the BCKD complex (Suryawan *et al*., 1998). This favours the release of BCKAs rather than their complete oxidation and with the almost complete absence of hBCATm in the human liver and the relative abundance of the BCKD complex, it is probable that this is the site of oxidation (Hutson *et al*., 1978; Hutson *et al*., 1980; Hutson *et al*., 1981; Shinnick *et al*., 1976).

Sweatt *et al.,* (2004a) examined the expression of BCATc in the rat brain, focussing on the cerebellum and hippocampus, this work demonstrated that BCATc was only expressed in neurons of the adult rat brain, but this expression had differing cellular localisation depending on the neuron-type. In glutamatergic neurons such as granule cells of the cerebellar cortex and of the dentate gyrus BCATc was localised to axons and nerve terminals, and in GABAergic neurons such as cerebellar Purkinje cells and hippocampal pyramidal basket cells BCATc was concentrated in the cell body. Garcia-Espinosa *et al.,* (2007) performed a more widespread analysis of BCATc within the CNS and demonstrated that BCATc immunoreactivity was present in every major anatomical division of the brain, with only neurons expressing BCATc. Immunolabelling of glial cells or vascular elements was not observed, however

in the developing rat brain it was observed that BCATc expression was upregulated in neurons and glial cells as they respond to changes in connectivity and growth factors (Garcia-Espinosa *et al.*, 2007).

Although BCATc is localised predominantly in nervous tissue, accounting for 70% of rat brain BCAT activity, it has also been localised to the ovary and placenta (Hall *et al.*, 1993; Sweatt *et al.*, 2004[a,b]). The mitochondrial isoform was rarely mapped in these studies. Recent work by Cole *et al.,* (2012) finally mapped BCATm and BCKD to the rat brain where it was confirmed that BCATm was indeed present in mouse astrocytes and BCKD was present in neurons (Figure 1.5). However, BCATc has also been described at low levels in certain astrocyte populations in a human cell culture model that was not reported in rat models, therefore mouse and cell models may not be so directly applicable to humans (Bixel *et al*., 2001; Bixel *et al*., 1997).

1.6 The BCAA: BCKA shuttle

Localisation of BCATc to neuronal cells and BCATm to astrocytes led to the development of the BCAA: BCKA shuttle hypothesis. These accumulated expression studies, together with key metabolic studies, proposed that astrocyte transamination (via BCATm) was in the direction of glutamate and BKCA synthesis. The glutamate subsequently enters the glutamate-glutamine cycle and thus replenishes lost glutamate, whereas the BCKA is transported to the neuron to undertake the second half of the shuttle or further metabolised in astrocytes or neurons (via BCKD) (Cole *et al*., 2012). In neurons transamination (via BCATc) was in the direction of BCAA and αKG synthesis. The αKG from this reaction would contribute to the neuronal glutamate pool via

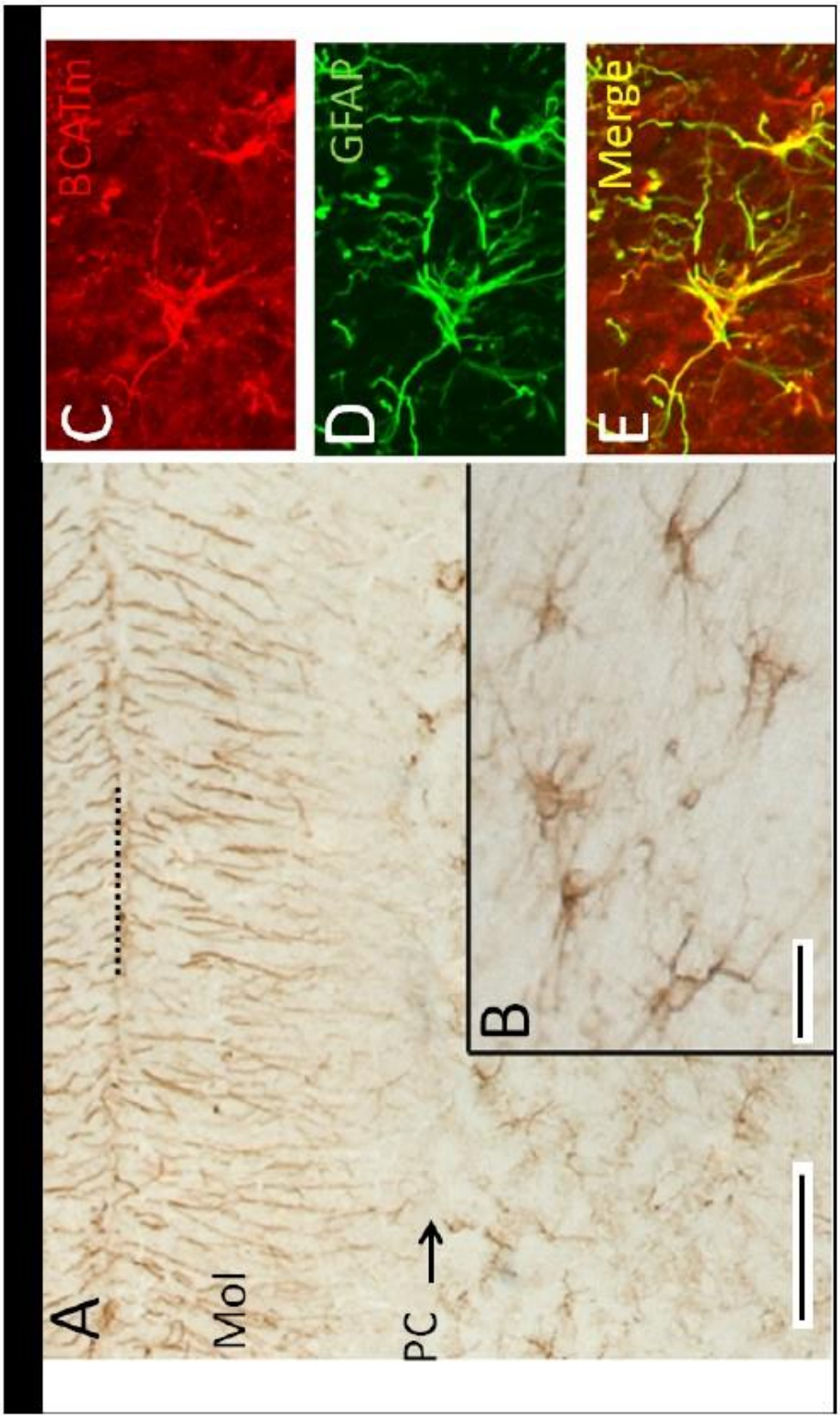

Figure 1. 5 Localisation of BCAT it current models. A: The presence of BCATm in the cerebellar cortex with presence in the molecular (MOL) and granule cell (GC) layer but not the purkinje cell (PC) layer. Dotted line refers to the pial surface. B: higher resolution of A showing clear astrocyte staining. C: rhodamine immunolabel of BCATm in the cerebellar white matter. D: fluoresceine-isothiocyanate-immunolabel of glial fibrillary acidic protein, a marker relatively specific to astrocytes. E: merged images of C and D. Scale bars: A 100 µm; B-E 25 µm (Cole *et al.*, 2012).

other means (i.e. GDH) or enter the Krebs cycle and the BCAA would decrease total nitrogen within the cell (Brand, 1981; Brookes, 1992; Chaplin *et al.*, 1976; Yudkoff *et al.*, 1994). These findings led to the development of the BCAA-BKCA shuttle hypothesis, which functions as an anapleurotic pathway alongside the glutamate-glutamine cycle to replenish 'lost' glutamate (Figure 1.6) (Yudkoff *et al.*, 1997; Hutson *et al.*, 2001). In fact, it has been demonstrated that 30% of *de novo* glutamate synthesis in rat neurons was produced by BCATc metabolism (LaNoue *et al*., 2001).

1.7 Leucine as a nutrient signal

The BCAAs (leucine, isoleucine and valine) are the most hydrophobic of all amino acids; this determines their role in protein formation (Creighton, 1993). For example, lung surfactant protein B is one of the most hydrophobic proteins and BCAAs make up 37% of the amino acid composition (Hawgood *et al*., 1998). Although they are similar in structure their role in metabolism varies, the end product of leucine catabolism is acetyl-CoA (ketogenic), valine catabolism is succinyl-CoA (glucogenic) and isoleucine catabolism is propionyl-CoA and Acetyl-CoA (both ketogenic and glucogenic) (Harper *et al*., 1984).

The effect of the BCAAs (particularly leucine) on protein production is well established (Nishitani *et al*., 2004; Stipanuk, 2007; Suryawan *et al*., 2011). However, the specific mechanism by which it activates protein synthesis is unclear. The effect appears to be insulin independent, although insulin levels are important for the maximal effect of leucine on protein production (Stipanuk, 2007). Leucine's effect is predominantly through activation of the mammalian target of rapamycin (mTOR) pathway, as leucine increases the phosphorylation

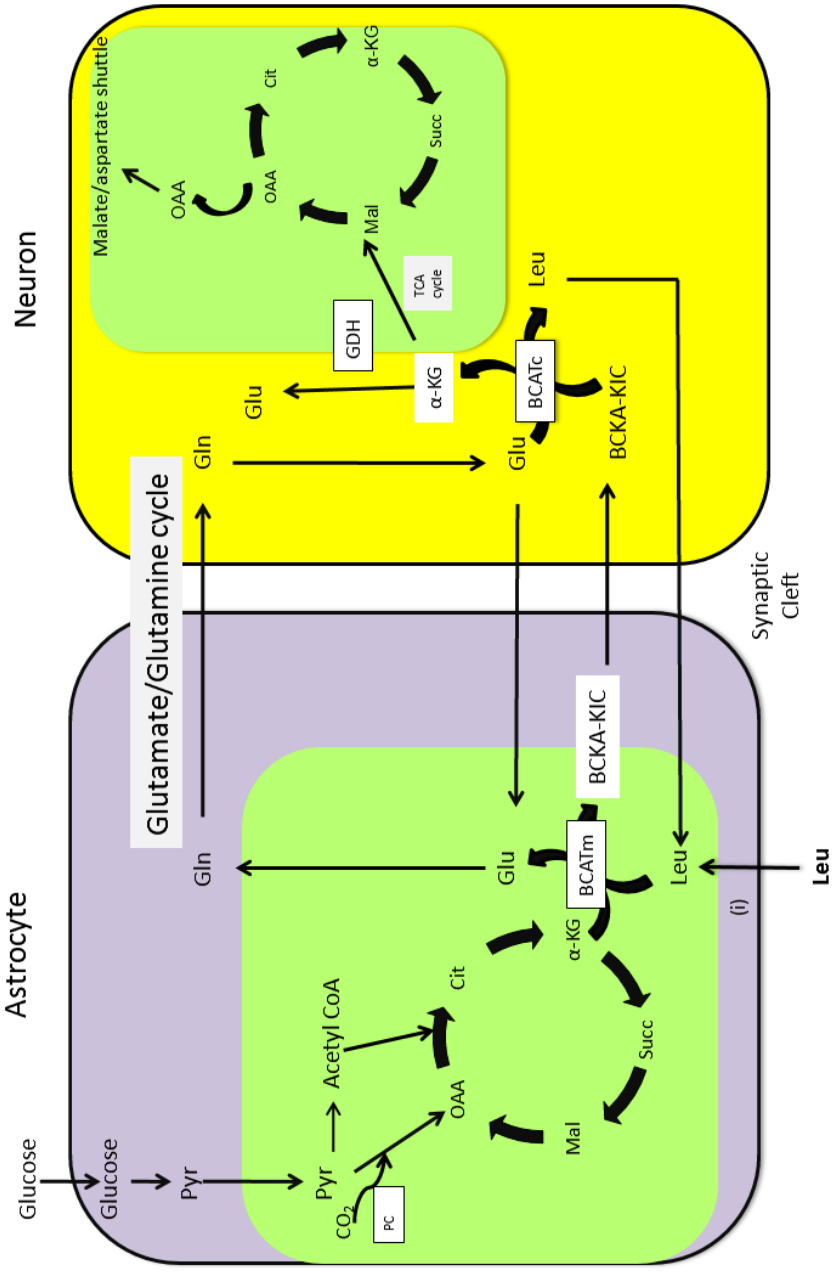

Figure 1. 6 Branched chain amino acid cycle and glutamate/glutamine cycle between astrocytes and neurons. Displayed is the branched chain amino acid cycle hypothesis that proposes that BCATm is the key producer of glutamate (out of BCATc and BCATm), and this glutamate is broken down to glutamine to be transported to the neuron where it is recycled to glutamate which is proposed to be used as a neurotransmitter or by BCATc to produce α-ketoglutarate for the Kreb's (or TCA) cycle. Green designates the mitochondria, purple designates the cytoplasm of the astrocyte, yellow designates the cytoplasm of the neuron (Conway *et al.*, 2012).

of mTOR and several other proteins associated with this pathway. However, leucine does not affect the upstream activities of mTOR and so is considered to effect mTOR through an 'insulin independent' mechanism (Figure 1.7) (Stipanuk, 2007). The mTOR protein is a large (290 kDa) serine/threonine protein kinase that modulates cellular growth, proliferation, autophagy and protein synthesis (Suryawan *et al*., 2011). The mTOR structure exists in two functionally distinct complexes, mTOR complex 1 (mTORC1) and mTOR complex 2 (mTORC2). It has recently been demonstrated that leucyl-tRNA synthetase (LTS) may couple intracellular leucine and mTOR signalling. The evidence for this is that mutations in the leucine binding residues of LTS render mTORC1 insensitive to intracellular leucine. After binding of leucine to LTS, it directly binds to Rag GTPase (an activator of mTORC1) by increasing localisation with Rheb.GTP (Min Han *et al*., 2012).

The effect of leucine on mTOR is not entirely removed upon rapamycin treatment (a potent inhibitor of mTORC1 signalling) implying additional mechanisms also operate to increase protein synthesis (reviewed by Nishitani *et al*., 2004). Supporting this is that in diabetic rats, leucine administration had no effect on mTOR signalling but nonetheless stimulated protein synthesis (reviewed by Stipanuk, 2007). Lynch *et al.,* (2002) demonstrated that norleucine was as effective as leucine in stimulating 4EBP1 phosphorylation. Conversely, Suryawan *et al.,* (2011) demonstrated that leucine and KIC (but not norleucine) enhanced the phosphorylation of 4E-binding protein 1 (4EBP1) (a marker of increased mTOR activity). It should be noted that both these experiments were performed in different models with Suryawan *et al.,* (2011) using pigs, and Lynch *et al.,* (2002) using rats.

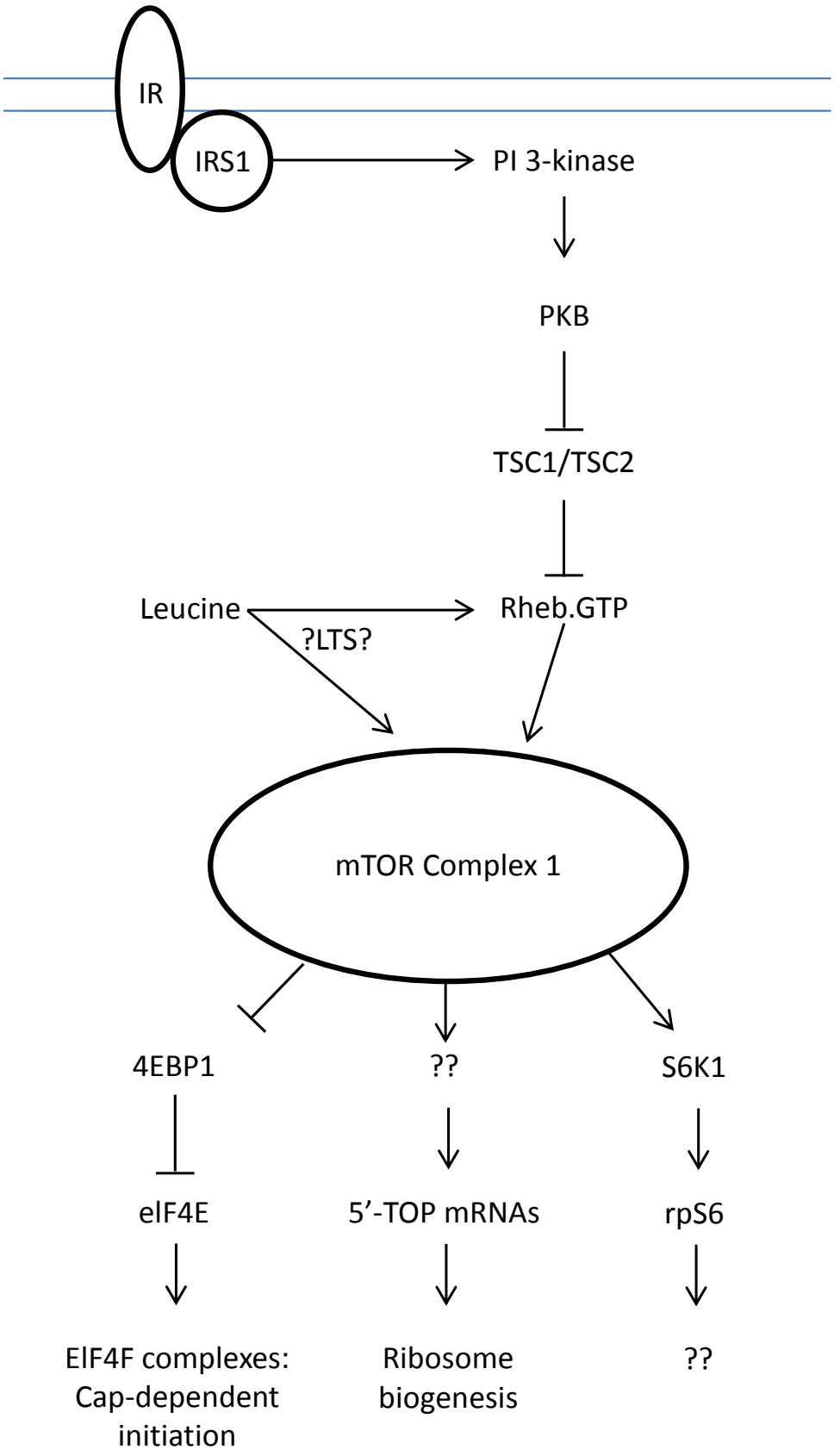

Figure 1. 7 mTOR activation via insulin receptor activation and the possible role of leucine. Activation of mTOR (by insulin) occurs through protein kinase B and the inactivation of tuberous sclerosis complex 1 and 2. It is currently proposed that leucine may act on mTORC1 via leucyl-tRNA synthetase (LTS) binding to Rag GTPase. This Rag GTPase (in the active conformation) interacts with Raptor, localizing mTORC1 to the surface of endosomes where Rheb.GTP is localized (acquired from Stipanuk, 2007).

It has been demonstrated that leucine and KIC are important secretagogues in insulin release. Leucine is firstly thought to stimulate insulin secretion through down regulation of surface adrenergic α2 receptors through the activation of the mTOR pathway. This down regulation decreases the ability of adrenaline to block insulin release (Yang *et al*., 2012). Other models have demonstrated that transamination of BKCAs are required to stimulate insulin secretion, which is blocked with the addition of BCAT inhibitors, implying a role for BCATm in this context (in addition to other occurrences of secretion) (Pizarro-Delgado *et al*., 2009; Zhou *et al*., 2010). It was therefore proposed that the effect of BKCA metabolism on insulin secretion directly correlated with the production of α-KG or leucine. However, current work on BCATm knockout mice observed that insulin secretion is in fact stimulated by both leucine and αKG separately. This proposes that leucine is either stimulating mTOR to increase insulin release or increasing the production of αKG through activation of glutamate dehydrogenase (Zhou *et al*., 2010).

1.8 The impact of BCAA in the pathology of disease

With the above association of BCAAs with key metabolic functions, associations with diseases such as diabetes, liver disease, sepsis and maple syrup urine disease (MSUD), their role in pathology and even in disease treatment has been extensively studied. However, it should be noted that although the studies were extensive in breadth many of the studies lacked appropriate depth and to date BCAA supplementation is rarely used for treatment in the United Kingdom.

1.8.1 Maple syrup urine disease

Mutations in the BCKD complex lead to the condition MSUD (Evarsson *et al*., 2000; Nellis & Danner, 2001). These mutations can occur in either the E1α (33%), E1β (38%) or the E2 gene (19%) with the best recognised mutations for MSUD also occurring in cell lines with an MSUD like pathology. For example cell line EM408 has a mutation in E1α (Y438N), EM1952 has mutations in E1β (N176Y/R324X) and EM3069 has a deletion in E2 (1031F 20kb deletion) (Nellis & Danner, 2001). This autosomal recessive disorder is characterised by the build-up of BCAAs and BKCAs that are neurotoxic to cells resulting in the patient presenting with symptoms such as neurological dysfunction and seizures, which can lead to infant death (Nellis & Danner, 2001). In MSUD a linear correlation is observed between levels of BCAAs and their corresponding BKCAs that are due to the uninhibited transamination of the BCAAs, with little or no further metabolism (oxidative decarboxylation) by the BCKD complex (Langenbeck *et al*., 1978). This disease demonstrates the importance of normal BCAA metabolism. It is worth noting that MSUD is the only 'model' for high BCAA exposure, which features substantial brain dysfunction but cannot serve as a realistic model for excessive BCAA exposure in normal healthy individuals.

1.8.2 Obesity and type II diabetes

Obesity and type II diabetes display a gradual increase in serum BCAAs and it is thought that this is an early event in type II diabetes pathology. This is due to the BCAAs having particularly sensitivity to the inhibitory effect of insulin on amino acid release from skeletal muscle - with growing insensitivity to insulin decreasing this inhibition of BCAA release (Lu *et al*., 2013). This is why in early

type II diabetes or obesity the levels of BCAAs are either normal or slightly elevated, despite the insulin resistant state. Adipose tissue is a significant contributor to BCAA metabolism and mitochondrial BCAA metabolism is significantly down regulated in adipose tissue of obese twins (compared to non-obese twins) (Pietilainen *et al*., 2008). This association of BCAAs and type II diabetes is further demonstrated by the elevated urinary excretion of BCAAs before insulin treatment and normalisation thereafter (Sasaki *et al*., 1988; Szabo *et al*., 1991). Further to this, in diabetic ketoacidosis, the plasma increase in BCAAs is large, returning to normal upon control of the disease (Adeva *et al*., 2012). This demonstrates a key role of the BCAAs in obesity and type II diabetic pathology in addition to a novel marker of disease progression.

1.8.3 Cancer

In bladder cancer, isoleucine and leucine have been demonstrated to be tumour promoters in rats by an increased agglutinability assay (Nishio *et al*., 1985). Furthermore, Sheen *et al*., (2011) demonstrated that melanoma cells were sensitive to leucine deprivation, which induced mitochondrial associated apoptosis (reviewed by Diaz-Meco, 2011). This result was repeated in glioma cells where leucine deprivation caused a growth arrest (Sheen *et al*., 2011; Takeuchi *et al*., 2011). Partially contradicting this research is the use of BCAAs in the suppression of hepatocellular carcinoma (in combination with angiotensin converting enzyme inhibitors). After curative therapy BCAA granules (12 g/day) and ACE inhibitors (perindopril 4 mg/day) decreased the cumulative recurrence rate by 50%. The mechanism is proposed to be related to improved insulin resistance and an anti-angiogenic property (Yoshiji *et al*., 2009; Yoshiji *et al*., 2011). Miuma *et al.,* (2012) demonstrated that BCAAs decreased the mRNA

stability of vascular endothelial growth factor, a key component in angiogenesis (Miuma *et al*., 2012). Even when used to treat hepatocellular carcinoma, BCAA supplementation rapidly improved liver function and Child-Pugh scores in patients who had undergone radiofrequency ablation (Morihara *et al*., 2012). It is probable that the role of BCAAs in carcinogenesis is type dependant in addition to timing dependent.

1.8.4 Liver disease

The BCAAs/tyrosine molar concentration ratio has been observed to correlate with markers of hepatic fibrosis, hepatic blood flow and hepatocyte function and were concluded to reflect the degree of hepatic impairment (Ishikawa *et al*., 2012). Supplementation has demonstrated efficacy in patients with liver cirrhosis; with large-scale trials in Italy and Japan demonstrating BCAA supplementation improves nutritional status, prognosis and quality of life (Muto *et al*., 2005). Similar supplementation favouring BCAAs has also demonstrated benefit to haemodialysis patients and the elderly by improving albumin and total protein levels (independent of dietary intake), while decreasing C-reactive protein levels and the risk of infection (Aquilani *et al*., 2011; Bolasco *et al*., 2011). Recent research into BCAA supplementation has demonstrated positive effects in the treatment of hepatic encephalopathy due to chronic liver disease, linking the BCAAs to cognition in humans (Afzal & Ahmad, 2010; Bak *et al*., 2013). However, the last Cochrane review (performed in 2002) of the subject failed to find an overall significance of BCAA supplementation on hepatic encephalopathy but commented on the poor methodology used in the trails at the time (Als-Nielsen *et al*., 2003).

The benefits of BCAA supplementation in these instances are through increased hepatic protein synthesis via stimulation of mTOR (although an mTOR independent effect on protein synthesis has also been proposed), stimulation of hepatocyte growth factor release, activation of glycogen synthase, increased glucose uptake in muscle tissue, improving glucose metabolism/insulin sensitivity, decreased risk of hepatocellular carcinoma and improved fatigue and sleep disturbances commonly associated with these diseases (reviewed by Kawaguchi *et al*., 2011; Khanna & Gopalan, 2007; reviewed by Nishitani *et al*., 2003).

1.8.5 Traumatic brain injury and Cognitive impairment

The neurological and cognitive effect of BCAA supplementation has not been studied in depth. Cole *et al.,* (2010) demonstrated that traumatic brain injury in mice observed significant reductions in hippocampal BCAAs and synaptic efficacy that were restored upon dietary consumption of a BCAA supplement. Mice that consumed BCAA supplement demonstrated greater cognitive improvement (Cole *et al*., 2010). In humans, BCAA supplementation was investigated in phenylketonuria and after a year of supplementation some improvements in cognition were noted (Berry *et al*., 1990). In hepatic cirrhosis, and the more severe chronic acquired hepatocerebral degeneration, supplementation markedly improved neurological signs and motor functions (Plauth *et al*., 1993; Ueki *et al*., 2001). BCAA supplements given to individuals with bipolar disorder, tardive dyskinesia and chronic obstructive pulmonary disease demonstrated a significant reduction in manic symptomology, involuntary motor movements and cognitive dysfunction as measured by the

mini mental state examination (MMSE) respectively (Scarna *et al*., 2003; Negro *et al*., 2010; Richardson *et al*., 2003).

The mechanism by which these effects are said to occur is thought to relate to transport across the blood brain barrier. The BCAA transport is shared with other large neutral amino acids, notably the aromatic amino acids, and is competitive in nature. It is proposed that some of these effects are (at least in part) due to this competition, with decreased aromatic amino acid transport leading to decreased serotonin (from tryptophan) and catecholamine (from tyrosine and phenylalanine) production (reviewed by Fernstrom *et al*., 2005). It has also been observed in cirrhotic patients that BCAA administration improved cerebral blood flow in certain regions (Iwasa *et al*., 2003; Yamamoto *et al*., 2005). It is likely that this may occur in other altered cognitive states.

1.8.6 Contraindication of BCAA supplementation

There are however, other studies that warn against such supplementation (De Simone *et al*., 2013; Piscopo *et al*., 2011). De Simone *et al.,* (2012) demonstrated that high BCAA medium given to microglial cells in culture exhibit a phenotype towards the M2 state with enhanced IL-10 expression, phagocytic activity and free radical generation along with a decreased neuroprotective function. It was proposed that these microglia would promote the establishment of a low grade chronic inflammation and increasing likelihood of neurodegeneration (De Simone *et al*., 2012). Studies in mice observed that BCAA administration significantly down regulated antioxidant genes while up regulating some oxygen transporters. It was concluded that BCAA administration could alter specific oxidative stress pathways which could be

detrimental in disease (Piscopo *et al*., 2011). Human studies with BCAA supplementation have tended to focus on amyotrophic lateral sclerosis (ALS), and so far no effect on the clinical progression of ALS has been observed conclusively (Ryberg *et al*., 2003; The Italian ALS group, 1993).

1.9 The BCAT proteins in health, disease and animal models

Alteration of glutamate metabolism is associated with Alzheimer's disease (AD), stroke and epilepsy. Despite this, the presence of BCAT has not been investigated in these diseases and disease models (Ascencio *et al.*, 1997; Benvenisty *et al.*, 1992). However, the limited work that has been done has observed some positive results, albeit lacking any depth to the association between the disease and the BCAT protein. For example, Nishimura *et al.,* (2013) demonstrated that expression of BCAT1 was a useful genomic biomarker for cardio-toxicity in rats, with BCAT1 expression increased both 8 and 24 hours post cardio-toxic event depending on the toxin used. It was proposed that this involvement was related to the role of BCATc in apoptosis (Eden & Benvenisty, 1999; Kholodilov *et al*., 2000; Nishimura *et al.*, 2013). Another example is from an animal model of nephrotic syndrome. In this model, kidney expression of BCATm was reduced 30% compared to that of control. It was proposed that in this model, catabolism of the BCAAs was decreased in order to conserve body nitrogen (Ascencio *et al.*, 1997).

1.9.1 Cancer

In rats, BCATm is extrahepatic in the adult, however it is highly expressed in the foetal liver which rapidly disappears after birth. It was demonstrated that BCATm was present not only in the immortal hepatic cell line AS-30D, but also

in the regenerating liver (with BCATm disappearing upon complete liver regeneration) (Perez-villasenor *et al*., 2005). This work follows from Ogawa and Ichihara (1972) that localised BCATc expression in rapidly proliferating poorly differentiated hepatomas, with benign tumours having an enzyme expression pattern much closer to healthy hepatocytes. The BCAT1 gene is highly expressed in early embryogenesis and is localised to the neural tube, the somites and mesonephrous during organogenesis and was first isolated in c-myc induced tumour (Benvenisty *et al.*, 1992).

Despite this the use of hBCATc inhibitors for the control of cancer is a recent occurrence (Benvenisty *et al*., 1992; Mclver *et al*., 2013; Radlwimmer *et al*., 2012[a,b]). Another recent patent from Radlwimmer *et al.,* (2013[a,b]) uses the measurement of hBCATc in the use for the diagnosis of brain tumours and gliomas, and the estimation of prognosis therein. It is described in the patent that tumours with an increased hBCATc expression have a poorer prognosis, and it is proposed that this patent will also find use in the prognosis for acute myeloid leukaemia (Radlwimmer *et al*., 2013[a,b]). Another 2013 patent by Rosenthal *et al*., has similarly patented the measurement of the BCAT1 gene in serum to detect colorectal cancer due to a 50% increase in mRNA expression in these patients (Rosenthal *et al*., 2013). Increased hBCATc has also been associated with papillary thyroid cancer, which was identified by gene expression analysis (Zhu *et al*., 2013). It is likely that this increased expression of hBCATc (at either the protein or mRNA level) is related to the c-myc regulation of this protein (Benvenisty *et al.*, 1992). Invasive testicular germ cell tumours can occur by a gain in copy number of the short arm of chromosome

12. This is the location of hBCATc, and is only expressed in embryonic carcinomas (McIver *et al*., 2013).

Prostate cancer has been associated with an intragenic hypomethylation of BCAT2 in Gleason score 7 versus Gleason score 8 (Kron *et al*., 2013). This implies that there is an increased hBCATm expression in these instances, however this was not further investigated. It is likely that the role of hBCATm in these instances is as an energy source, with the metabolism of BCAAs utilised to provide Kreb's cycle intermediates for the increased energy expenditure of proliferating cells. The role of hBCATc may possibly be the same but also may be due to the role in apoptosis and cell survival BCATc has been observed to have (Kholodilov *et al.*, 2000; Madeddu *et al*., 2004).

1.9.2 Knock-out mice

N-ethyl-N-nitrosurea mutagenesis produced homozygous deletion of exon 2, and produced a marked decrease in BCATm mRNA, presence and activity. The BCATm mutated mice displayed MSUD characteristics that responded to BCAA restriction with an amelioration of symptoms (Wu *et al*., 2004). There has recently been the further production of a stable BCATm knock-out mouse model (She *et al*., 2007[a,b]). This has been unmanageable so far for BCATc due to the role this protein has in neuronal development, with knock-out models incompatible with life. These BCATm knock-out mice displayed elevated serum BCAA levels, decreased adiposity and decreased body weight despite an increased appetite (attributed to the increased presence of orexigenic neuropeptides) (Purpera *et al.*, 2012).

Other work demonstrates that leucine suppresses food intake when administered to the brain or when supplemented in the diet (Blouet *et al*., 2009; Cota *et al*., 2006; Morrison *et al*., 2007; Newgard *et al*., 2009; Ropelle *et al*., 2008). It was concluded from the BCATm knockout mice studies that either BCAAs do not act as a nutrient signal or that transamination is required (by BCATm) for appetite suppression to occur (Purpera *et al*., 2012). These mice also demonstrated a markedly improved glucose and insulin tolerance along with an increased energy expenditure associated with a non-productive protein turnover (She *et al*., 2007 [a,b]). From this it was proposed that peripheral BCAA catabolism plays an important role in regulating insulin sensitivity (and therefore glucose levels) and energy expenditure.

1.9.3 Apoptosis

The role of BCATc in apoptosis seems to depend on the model used. Visual cortex ablation induced death of the neurons of dorsal lateral geniculate nucleus and was saved by BDNF treatment; this was mediated by an upregulation of BCATc (Madeddu *et al*., 2004). Kholodilov *et al.,* (2000) demonstrated that upon lesion formation in the substantia nigra, BCATc mRNA was upregulated in neurons. These neurons appeared normal in morphology and rarely contained apoptotic chromatin, so it was concluded that the presence of BCATc was maintaining viability in these cells (Kholodilov *et al.*, 2000). Conversely, utilising NIH/3T3 cells it was demonstrated that BCATc has a growth inhibitory effect and can promote apoptosis via glutamate, KIC and other BCKAs (Eden & Benvenisty, 1999). With the role hBCATc has in apoptosis and the role hBCATm has in glutamate production, it was proposed that alterations may

occur to these proteins in diseases where cell death and glutamate are a pathological mechanism.

1.10 Glutamate signalling and toxicity

Glutamate is the major excitatory neurotransmitter of the mammalian central nervous system and is involved in memory, learning and cognition but also plays a major role in the development of the central nervous system including cell migration, differentiation and synapse formation (Danbolt, 2001). Depending on the region, the brain concentration of glutamate is 5-15 mM with the majority of this localised inside nerve terminals. However, the extracellular concentrations in the brain and CSF are 3-4 µM and 10 µM, respectively (Hamberger *et al*., 1983; Hamberger & Nystrom, 1984; Lehmann *et al*., 1983; Schousboe, 1981).

The *de novo* synthesis of glutamate predominantly involves glutaminase, amino acid transaminases and enzymes of the Krebs cycle (in the form of α-KG) (LaNoue *et al.*, 2001). However, the synthesis of glutamate requires a nitrogen group in the form of ammonia, aspartate or the BCAAs. The BCAAs can cross the blood brain barrier, where the influx of leucine is considerably higher than other amino acids (Smith *et al.*, 1987; Oldendorf, 1973). Studies with [^{15}N] leucine have demonstrated that the BCAAs are nitrogen donors for the synthesis of glutamate and glutamine in brain explants and in primary neuronal cultures (Hertz *et al.*, 1987; LaNoue *et al.*, 2001; Yudkoff *et al.*, 1983; Yudkoff *et al.*, 1996). From *ex vivo* retinas and *in vivo* rat brain in addition to astroglial and neuronal cells in primary culture, it was demonstrated that *de novo* synthesis of glutamate was necessary for maintaining cellular levels of glutamate (LaNoue *et*

al., 2001; Gamberino *et al.*, 1997; Waagepetersen *et al.*, 2001).

The glutamate-glutamine cycle is the sequence of events that describe glutamate neurotransmission and signal termination within the brain. Firstly, action termination of glutamate is performed by the removal of glutamate from receptor sites by transport into astrocytes via glutamate transporters such as excitatory amino acid transporter (EAAT) 1 and EAAT2. Glutamate is subsequently metabolised to the relatively physiologically inert glutamine by the enzyme glutamine synthetase. Subsequently, glutamine is shuttled to excitatory nerve terminals, where it is converted back to glutamate by the enzyme phosphate activated glutaminase. This restored glutamate requires physiological storage in synaptic vesicles which is performed with the aid of vesicular glutamate transporters (Walton & Dodd, 2007). This process is not isolated, so small amounts of glutamate and glutamine are further metabolised for use in other pathways, such as the Kreb's cycle. Previously discussed research proposes that this 'loss' of glutamate is compensated for by the action of glutamate producing enzymes such as BCAT (Hutson *et al.,* 2001; LaNoue *et al*., 2001).

Despite the vital role of glutamate in neurotransmission, the systemic or intracranial administration of glutamate (or analogues) causes seizures, neuronal loss and glial activation (Hayashi, 1954; Lucas & Newhouse, 1957; Olney *et al.*, 1972; Ben-Ari, 1985; Olney *et al.*, 1986). This lead to the hypothesis that in certain diseases glutamate production could be increased or glutamate removal could be decreased to cause a process referred to as glutamate toxicity. Glutamate toxicity is the excessive stimulation of excitatory

glutamate receptors (predominantly NMDA receptors) due to the increased presence of glutamate in the synaptic cleft, causing a prolonged post-synaptic influx of sodium and calcium ions (Dong *et al.,* 2009; Hynd *et al.,* 2004; Arundine & Tymianski, 2003). The calcium ions eventually exceed the capacity of the regulatory mechanisms, which produces an inappropriate activation of calcium dependent enzymes and processes (Figure 1.8). These enzymes include proteases such as calpain, or synthases such as nitric oxide synthase. These bring about processes that directly damage neurons by cytoskeletal breakdown or toxic reaction product formation, like peroxynitrite ($ONOO^-$), that ultimately lead to cell death (Olney, 1978[a,b,c]; Rothstein, 1996; reviewed by Sattler & Tymianski, 2000). The sodium ions entering the neuron bring about osmotic damage due to the influx of chloride ions and water that swell the cell and interfere with signalling (Olney, 1978[a,b,c]; Olney, 1994; Lau & Tymianski, 2010).

It is not yet clear what initiates this excess glutamate signalling but current evidence supports the role of impaired cellular energy metabolism or abnormal activation of excitatory amino acid receptors occurring in a particular subpopulation of neurons (Albin *et al*., 1992). Levels of glutamate were demonstrated to be universally decreased in all areas of the cerebral cortex in AD, although this is considered to be related to the metabolic equivalent of glutamate rather than neurotransmission. This is in contrast to similarly decreased GABA levels which are thought to be both related to the metabolic and signalling role due to the decreased use of GABA as a metabolite (Ellison *et al*., 1986). The role of glutamate in toxicity is further supported by *in vitro* evidence that demonstrated glutamate toxicity enhances tau gene expression in

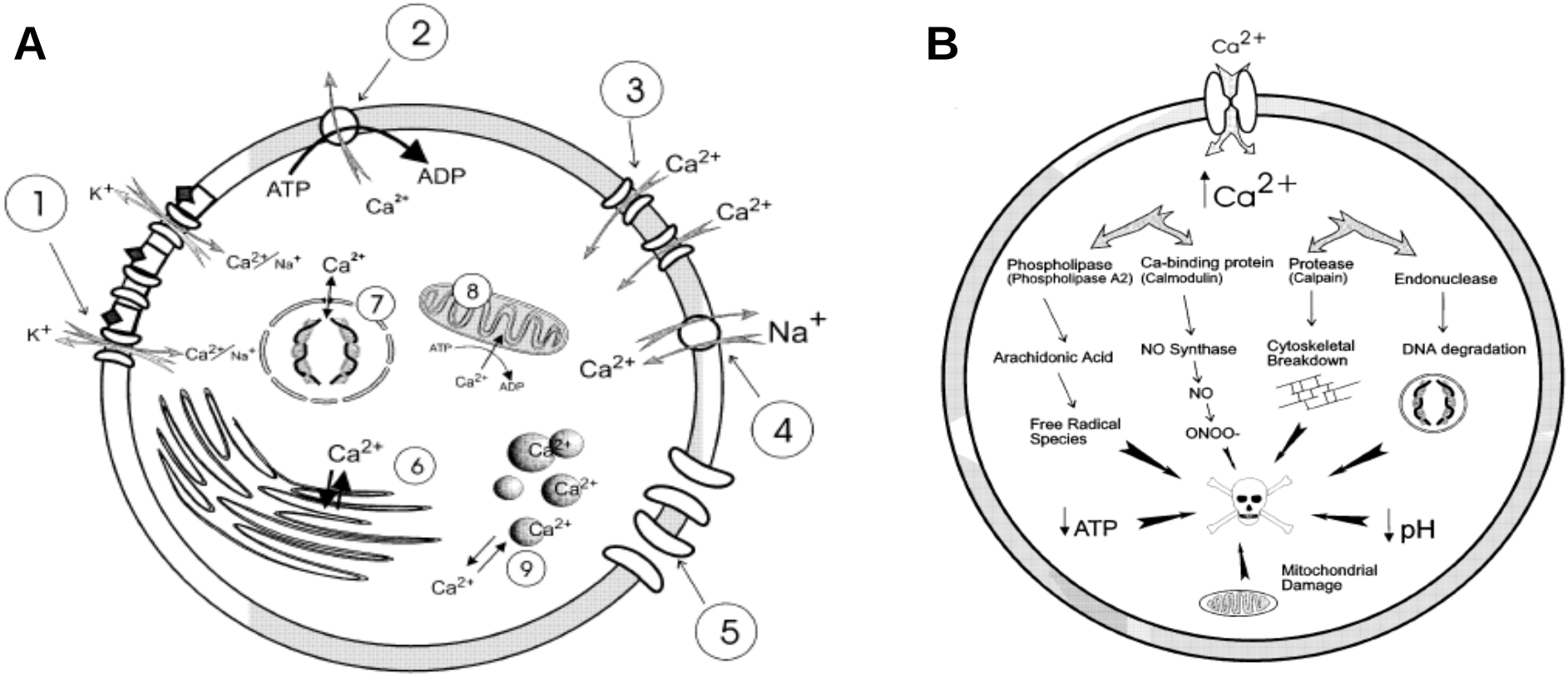

Figure 1. 8 An overview of glutamate toxicity. Figure A shows normal events of calcium homeostasis within the neuron. (1) Ca^{2+} and Na^{+} influx along with K^{+} efflux in receptor gated ion channels; (2) Ca^{2+} efflux via an ATP-requiring ionic pump; (3) Ca^{2+} influx via voltage-gated Ca^{2+} channels; (4) Ca^{2+} efflux via Na^{+}/Ca^{2+} exchanger; (5) additional ionic channels contributing to membrane repolarisation and ionic homeostasis; (6) Ca^{2+} sequestration (and release) by endoplasmic reticulum; (7) Ca^{2+} fluxes through the nuclear membrane with potential effects on nucleic acid transcription; (8) Ca^{2+} sequestration by mitochondria; (9) intracellular Ca^{2+} buffering by Ca^{2+}-binding proteins. Figure B shows how intracellular calcium increases lead to calcium dependent secondary phenomena that eventually lead to cell death. The intracellular increase in calcium required for the toxic activation shown above will only occur when regulatory mechanisms are overwhelmed, such as those described in Figure A (Sattler & Tymianski, 2000).

neuronal cultures and exacerbates amyloid β1-42 induced impairment of long term potentiation (Esclaire *et al*., 1997; Nakagami & Oda 2002).

Glutamate toxicity is closely linked with APP processing and Aβ production, in addition to tau hyperphosphorylation and tau pathology propagation. It is unclear which is the initial pathology in AD, whether they occur simultaneously or whether each may be an initiating pathology in its own right under varying conditions. For the example of amyloid, multiple fragments of Aβ (Aβ25-35, Aβ1-40 and Aβ1-42) potentiate glutamate release from hippocampal and neocortex neurons as well as inhibit glutamate removal from the synaptic cleft (Arias *et al*., 1996; Lauderback *et al*., 2001; Revett *et al*., 2013). In support of this, chronic administration of nano molar concentrations of Aβ oligomers induce NMDA receptor mediated calcium influx and mitochondrial calcium overload leading to cell death in hippocampal cultures (i.e. excitotoxicity) – this process is inhibited by Memantine (Alberdi *et al*., 2010; Bieshke *et al*., 2011). Many other studies have demonstrated that the pathological effects of Aβ in models of dementia are largely or completely removed by the presence of NMDA inhibition and exacerbated by even sub threshold levels of glutamate (Alberdi *et al*., 2010; Cowburn *et al*., 1997; De Felice *et al*., 2007; Klyubin *et al*., 2011; Li *et al*., 2009; Nakagami & Oda, 2002; Wei *et al*., 2010).

Prolonged activation of extra synaptic NMDA receptors has been reported to increase the neuronal production of amyloidogenic Aβ, whereas synaptic NMDA receptors promote non-amyloidogenic α-secretase mediated APP processing (Bordji *et al*., 2010; Hoey *et al*., 2009). Therefore, while Aβ can cause pathological NMDA activation, NMDA activation can in turn cause pathological

Aβ production. Also, a major caveat in amyloid initiated toxicity is that amyloid burden does not correlate with clinical severity of AD. In some cases AD pathology can be traced to areas that are amyloid free, or high amyloid deposition can occur in areas that are unaffected upon mental state examination (Tang *et al*., 2009).

A link between glutamate toxicity and tau phosphorylation was proposed when the treatment of rat hippocampal neurons with excess glutamate resulted in the labelling of these neurons for neurofibrillary tangles, as seen in AD (Mattson, 1990). Since then it has been demonstrated that excitotoxic NMDA activation (50 μM glutamate) increases tau production and increases tau phosphorylation via GSK-3β and CDK5 (Couratier *et al*., 1996; Esclaire *et al*., 1997; Hernandez *et al*., 2009; Lesort *et al*., 1999; Pizzi *et al*., 1995; Sindou *et al*., 1992). When this increase in tau production (with an anti-sense tau oligonucleotide) was inhibited, glutamate induced excitotoxicity did not occur (Pizzi *et al*., 1995). The splice variants of glutamate transporter EAAT2 are associated closely with tau pathology and even precede it, suggesting that glutamate pathology precedes tau pathology (Scott *et al*., 2010).

However, Clavaguera *et al.* (2009) demonstrated that injection of mutant tau into wild type mice induced tau pathology that spread from the site of injection to adjacent brain regions (Clavaguera *et al*., 2009). This demonstrates that while glutamate pathology may be capable of initiating tau pathology, tau pathology on its own is sufficient for pathology propagation. This mechanism of tau propagation was initially proposed to be due to neuronal death releasing hyper phosphorylated tau. However an additional mechanism has been

proposed in which glutamate stimulation of neuronal activity causes a release of tau from healthy mature cortical neurons. This in turn allows propagation of tau pathology from one cell to another and would explain the well documented progressive nature of tau pathology (Pooler *et al*., 2013).

Glutamate toxicity is further implicated in the pathogenesis and neuronal loss associated with many neurological disorders including epilepsy, stroke, Huntington's disease, fronto-temporal dementia, Parkinson's disease, temporal lobe epilepsy, ALS and AD (Greenamyre *et al.,* 1988). The largest evidence for glutamates role in disease is temporal lobe epilepsy, where phosphate activated glutaminase mRNA expression was increased by more than 100% in the subiculum in both patients with and without sclerosis. Glutamine synthetase mRNA expression was also increased by approximately 50% in the CA3 of temporal lobe epilepsy patients without hippocampal sclerosis compared with controls and patients with sclerosis (Eid *et al.*, 2012). Furthermore, patients with temporal lobe epilepsy have remarkably high concentrations of extracellular glutamate with this increasing markedly during a seizure (Cavus *et al.*, 2005; Cavus *et al.*, 2008; During & Spencer, 1993; Petroff *et al.*, 2004). It is unclear whether this increase in expression of two key glutamate handling enzymes was a protective or pathogenic event, but it lead to the hypothesis that the hBCAT proteins may too be upregulated in diseases where glutamate toxicity is considered a pathological mechanism such as AD.

1.11 Alzheimer's disease

AD is an age-related, neurodegenerative disease of the central-nervous-system associated with progressive cognitive impairment, memory loss and emotional

disruption (Parihar & Hemnani, 2004; Sultana & Butterfield, 2010). It is the most common cause of dementia accounting for 60-80% of all dementia, with the annual cost of dementia to the United Kingdom economy of £23 billion – more than cancer, stroke and heart disease (Desai & Grassberg, 2005; Luengo-Fernandez *et al.,* 2010; Walton & Dodd, 2007). Based on current trends a quadrupling of AD sufferers by 2050 is expected, bringing those suffering from AD to 106 million, leaving 1 in every 85 people with the disease (Brookmeyer *et al.,* 2007). Between the years of 1990 and 2010 AD went from the 24th largest cause of years of life lost to the 10th in the United Kingdom, and is the 7th leading cause of death in the USA (Heron *et al*., 2008; Murray *et al*., 2010). Current treatments of AD include cholinesterase inhibitors (donepezil, rivastigmine, galantamine) and Memantine (an uncompetitive NMDA antagonist) which do not reverse the effects of the disease, nor do they increase the life expectancy of the patient, however they temporarily slow the worsening of symptoms for 6 to 12 months in approximately half the individuals who take them (Birks, 2012; Winblad *et al.*, 2007; Alzheimer's Association, 2010).

The cause of AD is only known in a small population (<3%) of sufferers and is usually due to autosomal dominant mutation in the amyloid precursor protein gene or the presenilin genes 1 and 2. So far molecular genetics has only revealed risk factors for sporadic AD in the form of alipoprotein E (APOE), BIN1, CLU, CR1 and PICALM genotype (Bertram *et al*., 2010). The strongest association is with the APOE genotype, the ε4 genotype associated with an increased risk of AD by approximately 4-fold (reviewed by Brouwers *et al*., 2008). It is worth noting that a mutation in the Tau gene also causes dementia

but these dementias (referred to as tauopathies) are not associated with amyloid deposition (Buee & Delacourte, 2001; Hutton, 2000). Other risk factors associated with AD are age (increasing age increases likelihood), family history of dementia (history of two or more AD sufferers increases relative risk to 1.59), smoking (increases relative risk to 1.74) and previous education (less than eight years increases relative risk to 2.0) (Launer *et al*., 2007).

In health, 90% of amyloid present is in the form of Aβ40, and 10% in the form of Aβ42. The α-, β- and γ-secretases are proteases for the amyloid precursor protein (Esch *et al*., 1990). In health, the α-secretase cleaves the external part of the amyloid precursor protein with the γ-secretase cleaving the intramembrane site, producing Aβ40. In AD, cleavage occurs by β-secretase over α-secretase and Aβ42 is produced. It is this Aβ42 that makes up the majority of the amyloid present in plaques due to the more hydrophobic nature of the peptide (Iwatsubo *et al*., 1994). Down's syndrome (trisomy 21) is associated with dementia pathology identical to that of AD. This is due to the fact that the amyloid precursor protein gene is located on chromosome 21 and the additional copy seems to be responsible for this AD pathology (Wisniewski *et al*., 1985).

Tau functions in neurons (where it is predominantly expressed) to stabilise microtubules where it assists in axonal transport (Reviewed by Spires-Jones *et al*., 2009). Some proteins (such as kinesin) detach once they reach an area of high concentrations of bound tau, whereas others (such as dynein) reverse in direction (Dixit *et al*., 2008). In this context, kinesin will bind to microtubules and be transported to the synapse, where it will unbind due to the higher tau

concentrations and dynein will not be inhibited in the transport back to the cell body (Reviewed by Spires-Jones *et al*., 2009). Thus, tau can alter axonal transport of proteins in a mechanism independent of protein concentration. This binding to microtubules is regulated through phosphorylation (although other modifications occur), with the phosphorylated form having less affinity to microtubules (reviewed by Ballatore *et al*., 2007).

In all tau containing disease (including AD, Pick's disease, Amyotrophic lateral sclerosis, Creutzfeldt-Jakob disease, Down's syndrome and fronto-temporal dementia linked to chromosome 17) tau becomes hyper phosphorylated and this brings about pathogenesis by disrupting cellular trafficking and transport in addition to encouraging tau aggregation (which further inhibits transport) (Lee *et al*., 2001). Mutations in the coding regions of tau cause dementias that rarely include amyloid pathology, for example fronto-temporal dementia linked to chromosome 17. These mutations can alter the binding of tau to microtubules, the ability of tau to form fibrils or the splicing necessary for tau function (Boeve *et al*., 2008; Goedert *et al*., 2006).

1.12 Neuroanatomy and Neuropathology

The function of the various regions of the human brain is important in understanding the associated symptoms with progression of AD (Figure 1.9). The hippocampus is important for short term and long term memory in addition to spatial awareness, the temporal lobe is involved in auditory perception in addition to the semantics of speech and vision, the frontal lobe is associated with attention, long term memory and drive; and finally the parietal lobe integrates sensory information, particularly spatial sense and navigation (Aboitiz

Figure 1. 9 Brain sagittal section showing all main areas. A: the frontal lobe, mainly involved in motor functions, attention, planning, reasoning and impulse control; B: the temporal lobe, mainly involved in sensory processing, memory and semantics; C: the parietal lobe, mainly involved in spatial awareness and touch processing; D: the occipital lobe, involved with vision; E: the cerebellum, mainly involved in motor control; F: the midbrain, mainly involved with the motor system and dopamine production; G: the pons, mainly involved in cerebral connections and autonomic functions; H: the medulla oblongata, mainly involved in cerebral connections and autonomic functions (image taken from http://library.med.utah.edu).

et al., 2003). This explains why memory loss is one of the first symptoms of AD and that symptoms progress to confusion, irritability, mood swings, language breakdown, the loss of semantics, long-term memory loss and progressive apathy as the disease pathology spreads across the brain destroying functional areas (Waldemar *et al*., 2007; Fox *et al*., 1999).

Braak staging is a standardised measure of tau related pathology in the human brain. It is a histological process performed on all post mortem brains received for dementia research (in this case The South West Dementia Brain Bank) and is a 0-VI category method that measures disease propagation through the brain, with 0 associated with no pathology and VI associated with complete AD pathology. Stages of the disease can be distinguished by the location of tangle-bearing neurons and the severity of changes (Figure 1.10, Figure 1.11) (Braak & Braak, 1991; Braak & Braak, 1995). Amyloid is not used in the staging of AD progression due to the high variability, not only between individuals but also between brain regions of the same individual (Braak & Braak, 1991).

Even though the progression of AD is well documented, little is known about the cause of these key pathological features in the majority of cases, or why some individuals develop AD while others do not, other than an accumulation of risk factors that give little insight on the potential cause or underlying pathology. It was the aim of this study to investigate the distribution of hBCATc and hBCATm in control and diseased human brains with established immunohistochemistry techniques, in addition to evaluate any expressional or distributional differences between the AD brain and age and gender matched controls with Western blot

analysis. From this, the study was going to continue to try and mimic the features observed in AD utilising cell lines and biochemistry techniques.

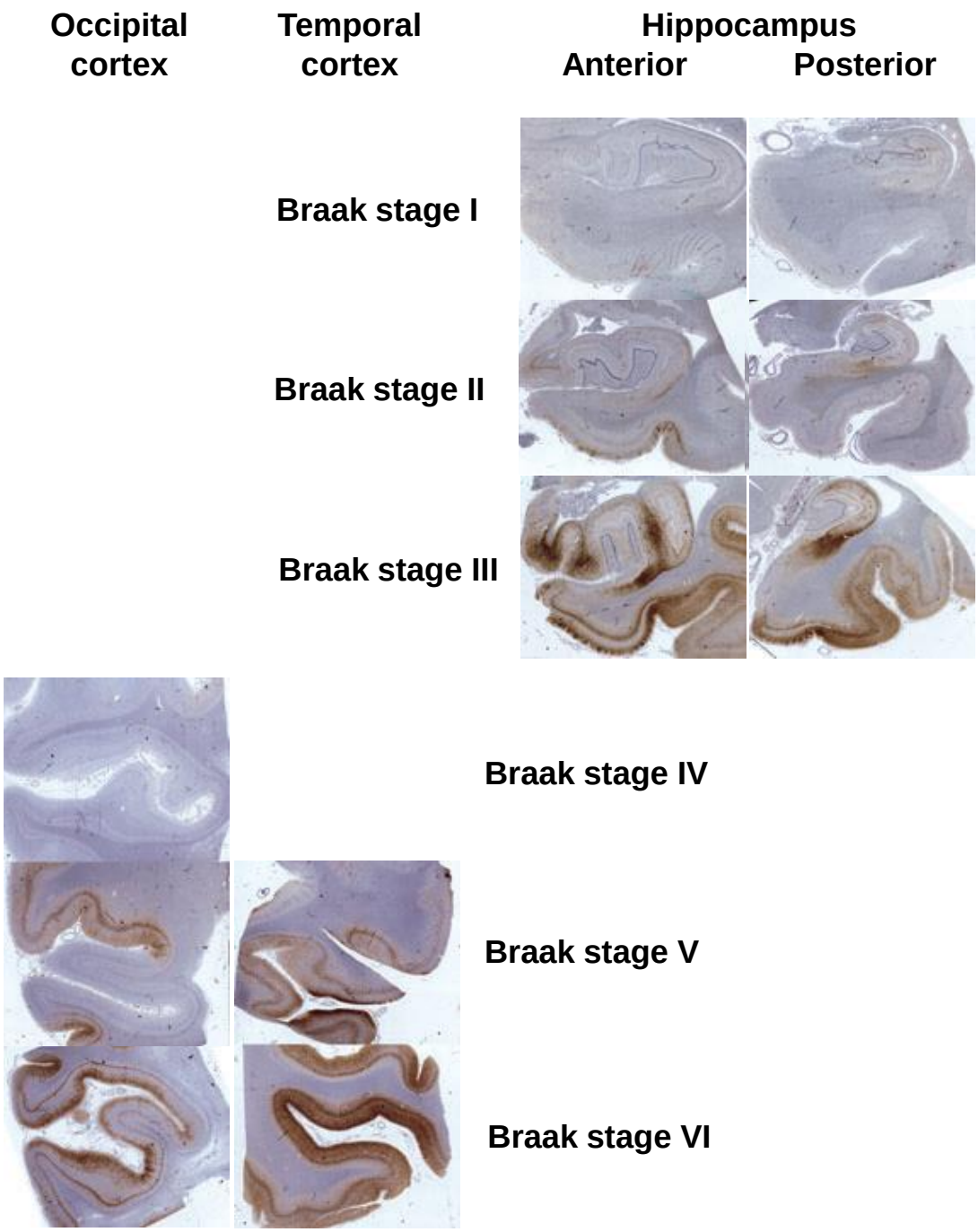

Figure 1. 10 Braak stages I-VI. Section from: occipital cortex including calcarine fissure; temporal cortex including middle temporal gyrus and at least a part of superior temporal gyrus; anterior hippocampus at the level of uncus; and posterior hippocampus at the level of lateral geniculate nucleus. It is shown that tau pathology initiates within the hippocampus and develops further into the temporal cortex and, at the later stages of the disease, into the occipital cortex (acquired from Alafuzoff *et al.*, 2008).

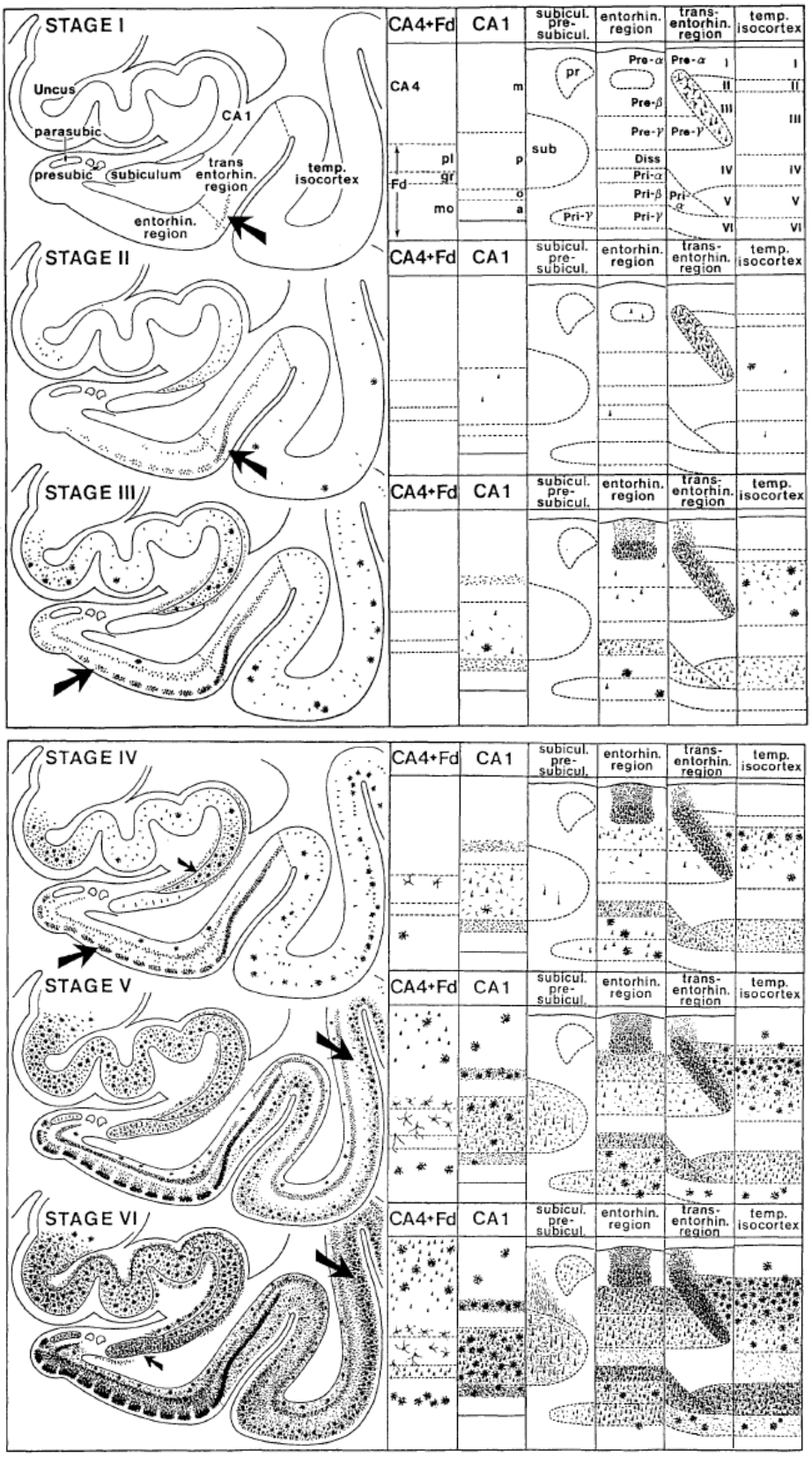

Figure 1. 11 A diagrammatic representation of hippocampus pathology with increasing Braak stage. It can be seen that the CA4 region of the hippocampus remains largely unaffected until the later stages of pathology. A diagnosis of AD requires a Braak stage of IV and above, with a diagnosis of definite AD occurring at Braak stage V and VI (acquired from Braak & Braak, 1991; Braak & Braak, 1995).

2 Aims and Objectives

Distribution

Hypothesis: It was the first hypothesis of this work that the distribution of the hBCAT proteins will be comparable between current animal models and the human brain.

Main Aim 1: Our aim in the present study was to examine the distribution of the BCAT proteins in the human brain, to ascertain whether the proposed BCAA-BCKA shuttle might contribute to the regulation of glutamate in the human brain. The regulation of glutamate is of particular importance for the prevention of excitotoxicity, an important contributor to neuronal cell death in brain ischemia and several neurodegenerative diseases. For the first time this study maps the BCAT proteins in the human brain. In contrast to reported findings in the rat brain, our findings highlight the presence of hBCATm in endothelial cells throughout the brain vasculature and an absence of detectable labelling in astrocytes. As in the rat, however, we report that in man hBCATc is restricted to neurons, although widely distributed throughout the brain. We discuss the impact of these findings with respect to the current BCAA-BCKA shuttle and offer an alternative mechanism for glutamate regulation in the human brain.

Expression

Hypothesis: It was the second hypothesis of this work that the expression of the hBCAT proteins will be altered in disease where glutamate is a pathological mechanism, such as AD.

Main aim 2: This study further aimed to investigate the expression and cellular distribution of hBCAT in the brains of patients with AD relative to matched control brains. Here, we provide the first evidence that both hBCATc and

hBCATm are upregulated in the hippocampus, frontal and temporal lobe in AD, and that this upregulation is occurring in different cell types. Not only was upregulation evident but we have also observe that there are potential variants of these proteins, indicating a post-translation modification event that alters proteins more in AD than in controls.

3 Materials

3.1 Antibodies

Mouse-raised antibody to protein disulphide isomerase (PDI – Ab2792) was purchased from Abcam (Cambridge, UK). 6 nm gold conjugated secondary antibody to mouse (DAM6/DAM10 nm 700.00) and 10 nm gold conjugated secondary antibody to rabbit (DAR6/DAR10 nm 700.000) were purchased from Aurion (Wageningen, The Netherlands). Mouse-raised antibody to glial fibrillary acidic protein (GFAP) and mouse-raised antibody to human leukocyte antigen-DR (HLA-DR) were purchased from DAKO (Cambridgeshire, UK). Rabbit-raised antibodies to hBCATc and rabbit-raised antibodies to hBCATm were raised against protein purified by this group and purchased from Insight Biotechnology limited (Wembley, UK). Mouse-raised antibody to AT8 (paired helical filament tau) was purchased from Innogenetics (Ghent, Belgium). Goat-raised Alexafluor 488 antibodies raised against mouse IgG (A-11031), goat-raised Alexafluor 568 antibodies raised against rabbit IgG and goat-raised Alexafluor 647 raised against rabbit IgG were purchased from Invitrogen (Paisley, UK). Mouse raised antibody to glyceraldehyde-3-phosphate dehydrogenase (GAPDH - SC-47724) was purchased from Santa Cruz (California, USA). Mouse-raised antibody to 4G8 (β-amyloid, 17-24) was purchased from Signet and distributed by Covance (Dedham, USA). Mouse antibody raised to glutathione was purchased from source bioscience (Nottingham, UK). Goat raised antibody to rabbit IgG (PI-1000) and horse raised antibody to mouse IgG (PI-2000) was purchased from Vector Labs (Peterborough, UK).

3.2 Chemicals

Electron microscopy (EM) grade gluteraldehyde was purchased from Agar (Essex, UK). L-[1-14C] Valine (0277) was purchased from American Radiolabelled Chemicals Inc. (MO, USA). 10% acetylated BSA (900.099) was purchased from Aurion (Wageningen, The Netherlands). EM grade paraformaldehyde was purchased from

BDH (Leicestershire, UK). Orthophosphoric acid (10173CD) was purchased from CTL (New York, USA). Acetic acid, anisole, AR acetone, copper sulphate, chloroform, dipotassium phosphate (K_2HPO_4), disodium-hydrogen-orthophosphate-dodecahydrate ($Na_2HPO_4.12H_2O$), ethylenediaminetertraaceteic acid (EDTA), ethylene glycol tetra acetic acid (EGTA), ethanol, glycerol (G/0650/17), glycine, glycogen, hydrochloric acid (H/1050/PB17), hydrogen peroxide, imidazole, isopropanol, Isopropyl β-D-1-thiogalactopyranoside (IPTG), methanol (M/4056/17), monopotassium phosphate (KH_2PO_4), N-ethylmorpholine (NEM - 149401000), potassium hydroxide (KOH), propidium iodide (PI - VXP3566), sodium bicarbonate ($NaHCO_3$), sodium chloride (NaCl - S/3160/65), sodium-dihydrogen-orthophosphate-dihydrate ($NaH_2PO_4.2H_2O$), sodium dodecyl sulphate (SDS - S/5200/53), sodium hydroxide (S/4920/60), sucrose, thiourea (T/1150/53), trifluoromethanesulfonic acid (TFMS), tris(hydroxymethyl)methylamine (tris - T/3710/60) and urea were purchased from Fisher scientific (Loughborough, UK). 3,3'-dihexyloxacarbocyanine ($DiOC_6$), ethidium bromide, kanamycin sulphate and ultrapure agarose (I6500-100) were purchased from Invitrogen (Paisley, UK). 3-[(3-cholamidopropyl) dimethylammonio]-1-propanesulfonate (CHAPS - C9526-5G), 4-(2-hydroxyethyl)-1-piperazineethanesulfonic acid (HEPES), 30% acrylamide (A3699-5X100ML), α-ketoisocaproate (KIC), β-mercaptoethanol, ammonium persulphate (A3678-25G), dithioltheirtol (DTT - D9779-5G), chloroform, dimethyl sulfoxide (DMSO), gabapentin (PHR1049-1G), glucose, hydrogen peroxide (H1009-100ML), iodacetamide (I6125-25G), memantine hydrochloride (M9292-25MG), phenylmethanesulfonylflouride (PMSF - 93482-50ML-F), poly-L-lysine, pyridoxal phosphate (PLP), sodium azide, sodium borahydride, sodium cocodelate, tetramethylethylenediamine (TEMED - T7024-25ML) and valproic acid sodium salt (P4543-10G) were purchased from Sigma-Aldrich (Dorset, UK). Uranylacetate was purchased from Taab (Reading, UK). Ethanol (20821.330) was purchased from VWR (Leicestershire, UK).

3.3 Molecular biology

Illford PQ universal developer (1757314) and Illford rapid fixer (1758285) were purchased from Avon film productions (Bath, UK). 4-20% Tris-HCl 10 well gels (161-1105) were purchased from BioRad (Hertfordshire, UK). Cover slips and glass slides were purchased from CellPath (Powys, UK). 6 well plates, 12 well plates, 15 mL Corning tubes, 50 mL Corning tubes, 96 well plates, T25 culture flasks and T75 culture flasks were purchased from Corning (London, UK). Human umbilical vascular endothelial cells (HUVECs) and IMR-32 cells were purchased from the European Collection of Cell Cultures (Salisbury, UK). Amersham hybond ECL nitrocellulose membrane (RPN78D), Amersham Hyperfilm ECL (28906836), ECL substrate (WBLUF0100), spectra ladder (PN26624), GelCode (PN24592), phosphate buffered saline (PBS) tablets (BR0014G), TWEEN 20 (233362500) and Whattmans blotting pads (CJF-240-090V) were purchased from Fisher scientific (Loughborough, UK). HiTRAP Q HP ion exchange column (17-1154-01) was purchased from GE healthcare (London, UK). RNase free tubes were purchased from Grenier Bio One (Gloucester, UK). 4-12% IPG gradient gels (NP0330BOX), 4-12% NuPAGE Novex bis/tris 10 well gel (NP0321BOX), 4x NuPAGE LDS sample buffer (NP0007), 10x sample reducing agent (NP0009), 20x NuPAGE MES SDS running buffer (NP0002), 20x NuPAGE MOPS SDS running buffer (NP0001), 20x NuPAGE transfer buffer (NP0006-1), carrier ampholytes (2M0021), IPG pH 4-7 gradient strips (ZM0012), IPG cassettes (ZM0003), NuPAGE antioxidant (NP0005), thrombin (Novagen), trypsin and tumour necrosis factor α (TNFα – GIBCO) were purchased from Invitrogen (Paisley, UK). EBM-2 and EGM-2 were purchased from Lonza (Slough, UK). Tryptone and yeast were purchased from Oxoid via Thermo Scientific (Hampshire, UK). Ni-NTA-agarose was purchased from Qiagen (West Sussex, UK). Bovine serum albumin (BSA - 700-100P) was purchased from Sera Labs (Crawley Down, UK). 100x glutamine, 100x penicillin-streptomycin solution, 100x RPMI amino acid solution, amyloid β fragment, aprotinin (A6279-5ML), brilliant blue G dye (B0770-25G), bromophenol blue (B8026-5G), dialysis

tubing, foetal calf serum, GBX developer (P7042-1GA), GBX fixer (P7167-1GA), interleukin 1α, interleukin 6, methylcellulose 25cp, non-essential amino acids (NEAA), protease inhibitor cocktail, RNAse free water, RPMI 1640 and Triton^{TM} X-100 (T8787-50ML) were purchased from Sigma-Aldrich (Dorset, UK). Haematoxylin, clearene and clearium were purchased from SurgiPath (Peterborough, UK). α-estradiol, β-estradiol, and testosterone were purchased from Tocris biosciences (Bristol, UK). DAPI containing mounting medium, donkey serum and Vectastain ABC kit containing avidin, biotin labelled secondary antibody to IgG, peroxidase substrate 3,3'-diaminobenzidine (DAB) and horse serum was purchased from Vector Labs (Peterborough, UK). Marvel was purchased commercially.

4 Methods

4.1 Tissue preparation of human brain samples for distribution and expression analysis

The study of the expression and distribution of hBCAT in the human brain was approved by North Somerset and South Bristol Research Ethics Committee. All brain tissue used in this study was from brains donated to the South West Dementia Brain Bank (SWDBB) at the University of Bristol. Tissue for the study of hBCAT expression in the MND brain was acquired as part of a pilot grant from the Medical Research Council (MRC) London neurodegenerative diseases brain bank.

Right cerebral hemisphere, half brainstem and half cerebellum were fixed in 10% buffered formalin for 3 weeks. Required tissue blocks were subsequently cut and paraffin embedded. Histological diagnosis was performed by a neuropathologist. A diagnosis of probable or definite AD was confirmed according to the Consortium to Establish a Registry for Alzheimer's Disease (CERAD) and Braak staging. Controls were diagnosed as those without AD or other neuropathological abnormalities, with an absence of clinical dementia.

For immunohistochemistry, sections 7 µm in thickness were cut from the temporal block encompassing the hippocampus, the para-hippocampal gyrus and the fusiform. For a proportion of individuals, sections of the cerebellum were also utilised as an internal control. For distributional analysis additional sections from the frontal, parietal and occipital lobes, basal ganglia, thalamus, hypothalamus, midbrain, pons and medulla were required. The cases used for the distributional analysis of hBCATc and hBCATm are reported in Table 4.1.

Table 4. 1 Control cases used in distributional analysis of hBCATc and hBCATm utilizing immunohistochemistry. All cases chosen had a PM delay of less than 48 hours and had no significant comorbidities (i.e. vascular dementia, Parkinson's disease, etc..). Case notes were read and all key details were noted.

Case	Age	Gender	PM delay (hours)	Brain weight (g)	Cause of death¥	Relevant illnesses§
Case 1	83	F	24	944	Ventricular failure	Non-specific colitis
Case 2	85	M	31	1337	Acute myocardial infarction	Neoplasm of prostate Heart disease
Case 3	87	M	24	1364	Acute renal failure	Hypertensive Myeloma
Case 4	78	M	48	NN	Prostate cancer	Hypertensive Chronic renal failure
Case 5	80	M	46	1279	Pneumonia	Hypertensive COPD
Case 6	73	M	35	1350	Bi ventricular heart failure	Hypertensive Heart disease
Case 7	88	F	28	1060	Pulmonary embolism	Rheumatoid arthritis
Case 8	72	F	24	1200	Age	NN
Case 9	89	F	15	1135	Serious fall	Rheumatoid arthritis
Case 10	80	F	39	750	Colon cancer	NN
Case 11	82	F	35	1150	Left ventricular failure	NN
Case 12	76	M	23	1450	Cardiac arrest	NN

Abbreviations: ADC – Alzheimer's disease case; CC – Control case; COPD – Chronic obstructive pulmonary disease; F – Female; M – Male; NN – None noted; PM – Post mortem.
¥ - Cause of death was determined at autopsy.
§ - Relevant illnesses contain any conditions mentioned suffered in the individuals life that appear in the case notes.

The cases used for immunohistochemical expressional analysis of hBCATc and hBCATm are reported in Table 4.2. The cases used for the distributional analysis of hPDI are reported in Table 4.3. All IHC labelling was performed simultaneously on both the disease and the matched control subject. After analysis of the entire cohort the samples were scored blind to the disease condition to ensure randomisation.

For Western blot analysis, temporal, frontal or motor cortex tissue (0.25 g) was homogenised in 1 mL of tissue homogenising buffer (1% SDS, 1 μM PMSF, 0.15 mM Aprotinin, 0.1 M NaCl, 10 mM Tris, pH 7.6) with silica beads and a Precellys 24 homogeniser (2x15 seconds). Post homogenisation the sample was centrifuged (8500 x g, 10 minutes, 4^{o}C). Following centrifugation, 50 μL aliquots of the supernatant were stored at -80^{o}C until analysis. The cases used for Western blot analysis of hBCATc and hBCATm in AD and control frontal and temporal cortex are reported in Table 4.4. The cases used for Western blot analysis of hBCATc and hBCATm in MND and control motor cortex are reported in Table 4.5. Western blots were performed on both the disease case and the matched control case on the same gel to remove gel to gel variability.

4.2 Immunohistochemistry

4.2.1 Investigation of hBCAT and PDI protein distribution within the human brain by Immunohistochemistry

Serial sections were placed in a 60^{o}C oven overnight prior to immunohistochemical staining to aid adhesion. Sections were dewaxed in clearene (2x5 minutes) and dehydrated in 100% ethanol (2x3 minutes). Endogenous peroxidase was quenched in 0.9% H_2O_2/methanol solution (30

Table 4. 2 Alzheimer's disease and control cases used in expressional analysis of hBCATc and hBCATm utilizing immunohistochemistry. All cases chosen had a PM delay of less than 72 hours, had no significant comorbidities (i.e. vascular dementia, Parkinson's disease, etc..) and were age and gender matched.

Case	Age	Sex	Braak	PM delay	Case	Age	Sex	Braak	PM delay
ADC 1	85	M	6	50	**CC 1**	85	M	2	31
ADC 2	95	F	5	28	**CC 2**	95	F	4	10
ADC 3	89	F	5	28	**CC 3**	89	F	3	47
ADC 4	86	F	5	72	**CC 4**	87	F	3	47
ADC 5	69	M	6	72	**CC 5**	69	M	2	66
ADC 6	65	M	5	39	**CC 6**	64	M	0	16
ADC 7	85	M	5	60	**CC 7**	86	M	3	16
ADC 8	95	M	4	27	**CC 8**	94	M	2	40
ADC 9	80	M	4	24	**CC 9**	80	M	0	46
ADC 10	88	F	6	64	**CC 10**	88	F	2	28
ADC 11	89	F	6	4	**CC 11**	89	F	2	15
ADC 12	80	F	5	51	**CC 12**	80	F	0	39
ADC 13	78	M	6	49	**CC 13**	77	M	1	42
ADC 14	87	M	6	36	**CC 14**	87	M	2	24
ADC 15	93	M	6	20	**CC 15**	93	M	3	38
ADC 16	74	M	5	24	**CC 16**	73	M	3	35
ADC 17	76	M	5	11	**CC 17**	76	M	2	23
ADC 18	78	M	6	50	**CC 18**	78	M	1	48
ADC 19	71	F	5	67	**CC 19**	72	F	0	24
ADC 20	74	F	6	12	**CC 20**	73	F	1	59
ADC 21	93	F	5	60	**CC 21**	93	F	1	15
ADC 22	73	M	5	17	**CC 22**	73	M	1	33
ADC 23	78	F	6	21	**CC 23**	78	F	1	22
ADC 24	69	M	5	12	**CC 24**	70	M	2	50
ADC 25	96	F	4	53	**CC 25**	94	F	2	21
ADC 26	79	M	6	28	**CC 26**	80	M	3	67
ADC 27	78	M	5	22	**CC 27**	78	M	2	12
ADC 28	88	M	5	3	**CC 28**	90	M	2	45
ADC 29	71	M	6	30	**CC 29**	71	M	1	25
ADC 30	83	F	5	5	**CC 30**	83	F	2	24

Abbreviations: ADC – Alzheimer's disease case; CC – Control case; F – Female; M – Male; PM – Post mortem.

Table 4. 3 Alzheimer's disease and control cases used in distributional analysis of hPDI with immunohistochemistry. All cases chosen had a PM delay of less than 72 hours and had no significant comorbidities (i.e. vascular dementia, Parkinson's disease, etc.). Case notes were read and all key details were noted.

Case	Age	Gender	PM delay (hours)	Brain weight (g)	Cause of death¥	Relevant illnesses§
AD case	86	F	72	1071	Bronchopneumonia Breast cancer	Essential hypertension
Control case	87	F	47	1262	Septicaemia COPD	Depression

Abbreviation: AD – Alzheimer's disease; COPD - Chronic obstructive pulmonary disease; F – Female; PM – Post mortem.
¥ - Cause of death was determined at autopsy.
§ - Relevant illnesses contain any conditions mentioned suffered in the individuals life that appears in the case notes.

Table 4. 4 Alzheimer's disease and control cases used in expressional analysis of hBCATc and hBCATm as analysed utilizing Western blot analysis. All cases chosen had a PM delay of less than 72 hours, had no significant comorbidities (i.e. vascular dementia, Parkinson's disease, etc..) and were age and gender matched.

Case	Age	Gender	Braak stage	PM delay (hrs.)	Case	Age	Gender	Braak stage	PM delay (hrs.)
ADC 1	95	M	4	27	**CC 1**	93	M	3	38
ADC 2	89	F	5	39	**CC 2**	88	F	0	72
ADC 3	88	F	6	64	**CC 3**	88	F	2	28
ADC 4	84	F	6	20.5	**CC 4**	84	F	1	17
ADC 5	80	M	4	24	**CC 5**	80	M	0	46
ADC 6	80	F	5	50	**CC 6**	80	F	0	92
ADC 7	69	M	6	72	**CC 7**	69	M	2	66
ADC 8	65	M	5	39	**CC 8**	64	M	0	16
ADC 9	86	F	5	73	**CC 9**	89	F	2	15
ADC 10	64	M	5	67	**CC 10**	64	M	2	12
ADC 11	70	F	6	25	**CC 11**	70	M	2	50
ADC 12	71	M	6	30	**CC 12**	71	M	1	25
ADC 13	71	F	5	67	**CC 13**	72	F	0	24
ADC 14	72	M	6	65	**CC 14**	72	M	1	42
ADC 15	73	M	5	17	**CC 15**	73	M	1	33
ADC 16	74	M	5	48	**CC 16**	73	M	2	36
ADC 17	74	M	5	50	**CC 17**	73	M	3	35
ADC 18	74	F	6	12	**CC 18**	73	F	1	59
ADC 19	74	M	5	24	**CC 19**	75	M	2	48
ADC 20	74	M	4	55	**CC 20**	75	M	3	6
ADC 21	91	M	3	43	**CC 21**	92	M	2	34
ADC 22	93	M	6	20	**CC 22**	94	M	2	40
ADC 23	83	F	5	5	**CC 23**	83	F	2	24
ADC 24	89	F	5	28	**CC 24**	89	F	3	47
ADC 25	96	F	4	53	**CC 25**	94	F	2	21
ADC 26	85	M	6	50	**CC 26**	85	M	2	31
ADC 27	76	M	5	11	**CC 27**	76	M	2	23
ADC 28	78	M	6	50	**CC 28**	78	M	1	48
ADC 29	78	M	5	22	**CC 29**	78	M	2	12
ADC 30	61	M	5	38	**CC 30**	62	M	0	4

Abbreviations: ADC – Alzheimer's disease case; CC – Control case; F – Female; hrs. – Hours; M – Male; PM – Post mortem.

Table 4. 5 Motor neuron disease and control cases used in expressional analysis of hBCATc and hBCATm as analysed utilizing Western blot analysis. All cases chosen had a PM delay of less than 72 hours, had no significant comorbidities (i.e. vascular dementia, Parkinson's disease, etc..) and were age and gender matched. It should be noted that although gender matching is ideal, the control cohort has an average age 4.4 years higher than the MND cases.

Case	Age	Gender	PM delay	Notes	Case	Age	Gender	PM delay	Notes
MNDC 1	78	M	2	MND	**CC 1**	78	M	24	Metastatic carcinoma
MNDC 2	72	M	26	MND	**CC 2**	81	M	18	Braak 1 - old cerebral infarct
MNDC 3	55	M	33	MND	**CC 3**	54	M	30	Control
MNDC 4	75	F	38	MND	**CC 4**	89	F	41	Control with CAA
MNDC 5	80	F	37	MND	**CC 5**	80	F	3	Minimal aging changes

Abbreviations: CC – Control case; CAA – Cerebral amyloid angiopathy; F – Female; M – Male; MNDC – Motor neuron disease case; PM – Post mortem.

minutes). Citrate buffer (120 mM trisodium citrate, pH 6.0) was used for antigen retrieval of tissue by bringing the citrate buffer to the boil twice and allowing to cool for 5 minutes and 15 minutes respectively. Slides were subsequently washed (2x3 minutes) in phosphate buffered saline (PBS – 0.154 M NaCl, 1.86 mM $NaH_2PO_4.12H_2O$, 7.48 mM $Na_2HPO_4.2H_2O$, pH 7.1) and blocked with 10% horse serum in PBS (20 minutes) to block non-specific binding sites. Primary antibody was prepared in PBS and incubation was performed overnight (20 hours) (rabbit polyclonal antibody raised to hPDI 1/500; rabbit polyclonal antibody raised to hBCATc 1/6000; rabbit polyclonal antibody raised to hBCATm 1/6000). Subsequent to overnight incubation the slides were washed in PBS (2x3 minutes) and a biotinylated antibody raised to IgG was applied (prepared as per Vectastain ABC kit instructions) (20 minutes). The slides were washed again in PBS (2x3 minutes) followed by application of avidin biotin complex in PBS (as per Vectastain ABC kit instructions) (20 minutes). Slides were washed in PBS (2x3 minutes), developed with DAB/H_2O_2 in distilled water (as per DAB substrate kit instructions) (10 minutes), washed in running water (10 minutes) and immersed in copper sulphate solution (16 mM $CuSO_4.5H_2O$, 0.123 M NaCl) (4 minutes). Sections were counterstained with Harris's haematoxylin (25% Gill haematoxylin) (30 seconds) and washed in running tap water (10 minutes). Finally, the sections were dehydrated in 100% ethanol (2x3 minutes), cleared in 100% clearene (2x5 minutes) and mounted in clearium.

Antibody specificity for antibodies purchased from Insight Biotechnology Ltd was tested by antigen absorption at 200x molar excess of antigen (either hBCATc or hBCATm). This showed that non-specific binding was not evident for hBCATc, but for hBCATm some granular staining of neurons was reduced

but not completely removed by antigen incubation. Sections were also probed with commercially available antibodies (Abcam) to compare tissue staining between antibodies. No difference in cell staining was observed between Abcam antibodies and Insight Biotechnology Ltd antibodies. Sections were viewed and scored on a Nikon Eclipse 50i microscope. Images were acquired with Simple PCI software and a QICAM colour 12-bit camera mounted on a Leica DM microscope.

4.2.2 Scoring protocol for expressional analysis of hBCAT in AD and control individuals

For anatomical reference, the sections were scored in the same locations on each slide: the collateral sulci of the temporal lobe and the overlying cortex and areas CA1 and CA4 of the hippocampus. These different regions were identified with the aid of a trained neuropathologist (where necessary) and Haematoxylin and eosin stained sections that were taken from all temporal blocks for post-mortem examination. Fields of vision were observed at 20x magnification; the area around the field of vision was also viewed. As the staining of hBCATm was much weaker than hBCATc, what constituted to ‘strongly stained’ was less. The scoring protocols for each brain area are fully described in Table 4.6, Table 4.7, Table 4.8, Table 4.9 and Table 4.10.

4.3 Wet transfer Western blot analysis

4.3.1 Protein concentration determination by the Bradford assay

For protein estimation a stock dye of Coomassie blue G was prepared (330 mg Coomassie blue G dye dissolved in 100 mL of phosphoric acid/ethanol (2:1) mixture). This was diluted to a working dye (3% stock dye, 3.8% ethanol, 8%

Table 4. 6 Non-neuronal staining scoring criteria for hBCATc and hBCATm utilizing immunohistochemistry

Non-neuronal staining score	Criteria
0	No non-neuronal staining of note.
1	<5 non-neuronal positively stained cells on average in a field of view in 20x magnification around the collateral sulci.
2	5-7 non-neuronal stained cells on average in a field of view in 20x magnification around the collateral sulci or <5 but with convincing non-neuronal stained cells also observed within the cortex surrounding the collateral sulci.
3	8+ non-neuronal stained cells on average in a field of view in 20x magnification around the collateral sulci or 5-7 but with substantial non-neuronal stained cells also observed within the cortex surrounding the collateral sulci.

Table 4. 7 hBCATc and hBCATm staining scoring criteria utilizing immunohistochemistry

Generic hBCAT staining score	Criteria
0	No hBCAT staining above background.
1	Incomplete, weakly stained neurons with or without minimal non-neuronal staining.
2	2 strongly stained neurons and either: • Less than the majority (but a significant amount) of neurons are medium stained. • Noticeable non-neuronal staining.
3	More than 2 strongly stained neurons and either: • Majority of neurons are medium stained. • Significant and intense non-neuronal staining.

Table 4. 8 Neuronal hBCATc and hBCATm staining score criteria for the CA4 area of the hippocampus and temporal area utilizing immunohistochemistry

hBCAT staining score	Criteria
0	No hBCAT staining above background.
1	Incomplete, weakly stained neurons.
2	1-2 strongly stained neurons and less than the majority (but a significant amount) of neurons are medium stained.
3	More than 2 strongly stained neurons with projections and majority of neurons are medium stained.

Table 4. 9 Neuronal hBCATc and hBCATm staining score criteria for CA1 area of the hippocampus utilizing immunohistochemistry

hBCAT staining score	Criteria
0	No hBCAT staining above background.
1	Neurons present are incomplete and weakly stained neurons.
2	Neurons present are medially stained.
3	Neurons present are greater than medially stained, or medially stained but present in a significant amount.

Table 4. 10 Blood vessel (BV) hBCATm staining scoring criteria utilizing immunohistochemistry

hBCATm staining score	Criteria
0	No hBCATm BV staining above background.
1	1-2 Clearly stained BVs, but BVs have largely low staining levels.
2	Most BVs are clearly stained with a few weakly stained BVs.
3	All BVs are clearly stained.

phosphoric acid) on the day of experimentation. A protein standard was prepared with purified BSA at a concentration of 1 µg/µL and was frozen down in 1 mL aliquots.

Appropriate dilutions (pure, 1/2, 1/5, 1/10, 1/15 or 1/20) of each sample were prepared and 5 µL of diluted sample was pipetted into triplicate wells. Working dye (200 µL) was pipetted into each well and the absorbance was measured at λ620 nm. The protein concentration was calculated utilising a standard curve produced by BSA protein (0.2 µg/µL to 1 µg/µL).

4.3.2 Wet transfer Western blot analysis

Protein samples at 1 µg/µL were prepared in loading dye and denatured at 95^{o}C (10 minutes). Proteins (20 µg) were separated on an SDS PAGE gels in electrophoresis buffer. The protein was transferred from the gel to nitrocellulose membrane at 35 V (20 hours) in transfer buffer (20% methanol, 20 mM tris, 152 mM glycine, 0.08% SDS, pH 8.3).

For the SNAP i.d. system (utilised in Western blot analysis of cell lysate and AD and control brain homogenate), post overnight transfer the membranes were washed with Tris buffered saline containing Tween (TBST – 0.1% TWEEN, 200 mM sodium chloride, 2 mM tris, pH 7.5) (3x10 mLs) blocked with 0.4 µm filtered 0.5% Marvel-TBST solution (30 mLs) prior to primary antibody incubation (10 minutes) (mouse monoclonal antibody raised to β actin 1/5,000, mouse monoclonal antibody raised to GAPDH 1/5,000, mouse monoclonal antibody raised to GSH 1/300, rabbit polyclonal antibody raised to hBCATc 1/3,000, rabbit polyclonal antibody raised to hBCATm 1/3,000) prior to TBST washing

(3x10 mLs). Horse radish peroxidase linked secondary antibody was subsequently added (10 minutes) (HRP linked goat polyclonal antibody raised to rabbit IgG 1/5,000, HRP linked horse polyclonal antibody raised to mouse IgG 1/5,000) prior to further TBST washes (3x10 mLs) and developed.

For antibodies that required overnight incubation (utilized in Western blot analysis of MND and control brain homogenate) the membranes were washed in TBST (3x10 minutes) prior to 5% marvel blocking (2 hours). Following block, the membranes were probed with the primary antibody (mouse monoclonal antibody raised to β-actin 1/10,000, mouse monoclonal antibody raised to GAPDH 1/20,000, rabbit polyclonal antibody raised to hBCATc 1/10,000; rabbit polyclonal antibody raised to hBCATm 1/5,000;) in 5% Marvel (in TBST) and remained at 4^{o}C overnight on a rocker prior to TBST washes (3x10 minutes). Horse radish peroxidase secondary antibody was subsequently added (HRP linked goat polyclonal antibody raised to rabbit IgG 1/10,000; HRP linked horse polyclonal antibody raised to mouse IgG 1/10,000) (1 hour). The membranes were washed again in TBST (3x10 minutes) and developed.

Membranes were developed utilizing horse radish peroxidase substrate (2 minutes) prior to film exposure (2 minutes) (developer time was always less than a minute and time in the fixer was maintained at 20 seconds). Image J was used to analyse the bands found via Western blot analysis and the densitometries were estimated relative to the loading control (either β-actin or GAPDH). This was tested for significance in Minitab (Section 5). For re-probing, membranes were incubated with 1 M NaOH (7 minutes) and washed in TBST (3x10 minutes). This was subsequently treated from blocking step.

If staining of the gel was required the gel was washed with deionised water (5 minutes) prior to the addition of GelCode and the gel was stained overnight. The gel was subsequently washed with water (4x10 minutes) to de-stain. If a detailed stain was required the gel was washed with deionised water (5 minutes) prior to fixation in 10% acetic acid and 50% methanol (1 hour). The gel was stained with brilliant blue G-colloidal concentrate (20% methanol, 2 hours), de-stained in 10% acetic acid and 25% methanol (60 seconds) and further de-stained in 25% methanol. This was imaged with a GelDoc.

4.3.4 Wet transfer Western blot analysis of cell lysate

Protein samples at were prepared in loading dye (4x bromophenol blue dye in 200 mM Tris, pH 6.8; 4x SDS-glycerol containing 40% glycerol and 8% SDS; 5% β-mercaptoethanol) and denatured. Proteins were separated on a 12% SDS PAGE gel (0.375 M Tris-HCl pH 8.8, 1% ammonium persulphate, 1% sodium dodecyl sulphate, 0.06% tetramethylethylenediamine, 12% acrylamide) in electrophoresis buffer (25 mM tris, 190 mM glycine, 0.1% SDS, pH 8.3) and transferred. The SNAP i.d. system was used to probe the membranes.

4.3.5 Wet transfer Western blot analysis of AD human brain homogenate

Protein samples at were prepared in loading dye (Invitrogen) containing 5% β-mercaptoethanol and denatured. Proteins (20 µg) were separated on a 4-20% Tris-HCl pre-cast gradient gel (Bio-Rad) at 150 V (1 hour) in electrophoresis buffer (25 mM tris, 190 mM glycine, 0.1% SDS, pH 8.3) prior to transfer. The SNAP i.d. system was used to probe the membranes.

4.3.6 Wet transfer Western blot analysis of MND human brain homogenate

Protein samples at were prepared in loading dye (Invitrogen) containing 5% β-mercaptoethanol and denatured. Proteins (20 µg) were separated on a 4-12% Tris-HCl pre-cast gradient gel (Invitrogen) at 100 V (1 hour) in electrophoresis buffer (Invitrogen) prior to transfer. Overnight incubations were used to probe the membranes.

4.4 Cell culture

4.4.1 Cell culture of human neuroblastoma IMR-32 cells

Cells were maintained in RPMI 1640 containing 10% foetal bovine serum, 1x RPMI 1640 amino acid solution, 1x glutamine and 1x penicillin-streptomycin solution (complete medium). For passage, the cells were washed in sterile filtered, autoclaved, PBS prior to trypsinisation (3 mLs of 1x trypsin for T75, 1 mL for T25, 0.5 mL for a single well of a 6 well plate) until all cells were detached from the flask. Trypsin was inactivated by the addition of an equal volume of complete medium and cells were centrifuged (5 minutes, 65 x g), re-suspended in complete medium, counted (utilizing a haemocytometer and 0.25% Trypan blue) and seeded as appropriate ($0.1x10^6$ cells/mL). Cells were stored and treated in humidified incubators set at 37^oC, 95% air and 5% CO_2.

For cell storage, $1\text{-}2x10^6$ cells were resuspended in 95% complete medium and 5% DMSO, brought to -80^oC overnight utilizing an isopropanol storage device and stored in liquid nitrogen. When resuscitated from liquid nitrogen, complete media in a T25 plate was equilibrated in an incubator for 30 minutes. Cells were rapidly defrosted in a 37^oC water bath and subsequently pipetted into the medium. Once cells had adhered (2 hours), the medium was changed to

remove remaining DMSO. Cells defrosted from liquid nitrogen were not used for experiments for at least 2 passages.

4.4.2 Treatment of IMR-32 cells for Western blot analysis, activity assay and flow cytometry

Undifferentiated IMR-32 cells (of passage lower than 30) were treated in serum deprived complete media (unless otherwise stated) at a confluence of between 60 and 70%. For treatments that did not require previous dilution, the substances were dissolved directly within the media (e.g. glutamate), maintained at 37^{o}C and sterile filtered prior to treatment. For treatments that required dilution, the substances were dissolved in manufacturer recommended solutions (e.g. 1% BSA in PBS for IL1α). All treatments were prepared on the day of use and not stored. The control treatment also received equal amounts of the recommended solution for dilution but without the active component. Table 4.11 gives an overview of the treatments used in experimentation and the buffers used in dilution (as per manufacturer's instruction). For protein extraction RIPA buffer was used (Method 4.4.3), for activity assays buffer B extraction buffer was used unless the buffers were the focus of the experiment, and for flow cytometry the cells were detached in the same manner as cell passage unless cell detachment was the focus of the experiment.

4.4.3 RIPA extraction of cell lines for expressional analysis

Cells were washed with ice-cold sterile PBS (3x) and extracted in RIPA buffer (10 mM Tris pH 7.6, 150 mM NaCl, 1 mM EDTA, 1 mM EGTA, 1% SDS, 1% protease inhibitor cocktail). The cells were scraped and incubated on ice (5 minutes). Samples were subsequently passed through a G21 needle 20 times

Table 4. 11 Cell treatments for IMR32 neuroblastoma cells.

Treatment	Dissolved/diluted in	Length of treatment	Experiment used in
2, 10, 12 and 20 mM Glutamate	Directly in media	30 minutes, 12 and 24 hours	Phase contrast microscopy Western blot analysis Flow cytometry Radioactivity assay
4, 8 and 12 mM Ketoisocaproate	Directly in media	24 and 72 hours	Phase contrast microscopy Western blot analysis
1 mM dibutyryl cAMP + 10 µg/mL Papaverine	Directly in media	8 days	Phase contrast microscopy Western blot analysis
10 µM retinoic acid	DMSO	8 days	Phase contrast microscopy Western blot analysis
10 µM retinoic acid + 1 mM dibutyryl cAMP	DMSO for retinoic acid Directly in media for dubutyryl cAMP	8 days	Phase contrast microscopy Western blot analysis
2 mM sodium butyrate	Directly in media	8 days	Phase contrast microscopy Western blot analysis
1 mM dibutyryl cAMP + 4 µM 5-bromo-2'-deoxyuridine	Directly in media for both	8 days	Phase contrast microscopy Western blot analysis
5, 20 and 40 mM leucine	Directly in media	24 hours	Flow cytometry Western blot analysis Radioactivity assay
0.01, 0.05, 0.20, 1.00, 2.00 and 5.00 ng/mL TNF alpha	Water at 0.5 mg/mL	24 hours	Western blot analysis Radioactivity assay
100 nM Insulin	125 mM $NaHCO_3$ at 1 mg/mL	24 hours	Western blot analysis Radioactivity assay
0.005, 0.01, 0.02, 0.10 and 1.00 ng/mL IL1 alpha	1% BSA in PBS	24 hours	Western blot analysis
0.2 and 2.0 ng/mL 17 beta oestradiol	1% BSA in PBS	24 hours	Western blot analysis

Abbreviations: BSA – bovine serum albumin; cAMP – cyclic adenosine 3′,5′-monophosphate; DMSO – dimethyl sulfoxide; IL – interleukin; PBS – phosphate buffered saline; TNF – tumour necrosis factor.

and again incubated on ice (30 minutes) prior to centrifugation (10,000 x g, 10 minutes, 4^{o}C). Following centrifugation, 50 µL aliquots of supernatant were stored at -20^{o}C until use.

4.4.4 Tissue extraction maintaining hBCAT activity from human neuroblastoma IMR-32 cells

Approximately 6x10^{6} cells were washed in sterile filtered PBS (3x, 4^{o}C) and scrapped into 250 µL of cell extraction buffer (Table 4.12). This was sonicated on ice (15 second sonication intervals, with 10 second periods on ice), prior to centrifugation (10 minutes, 10,000 x g, 4^{o}C). The activity of hBCAT in 200 µL of supernatant was assessed immediately.

4.5 Flow cytometry

4.5.1 Investigation of cell surface hBCATc expression by Flow cytometry

Cells were maintained as discussed in cell culture protocol (Method 4.4), and treated in the same manner (if treatment was required). All experiments had a secondary antibody only control to demonstrate the background fluorescence of the Alexafluor antibody, a cell only control to demonstrate the unaltered fluorescence of the cells and natural propidium iodide positivity of the cell population, and a cell only-half dead control as a positive control for propidium iodide fluorescence (cells incubated at 95^{o}C for 10 minutes, cooled on ice, diluted 50:50 with cell only control). Prior to flow cytometry, cells were detached with 1x Trypsin solution and 0.25 x10^{6} cells were centrifuged (5 minutes, 1400 x g for this and subsequent centrifugation), washed by re-suspending the cells in blocking buffer (1% BSA, 0.1% sodium azide in PBS) and centrifuged again. Cells were re-suspended in 200 µL of primary antibody solution (rabbit

Table 4. 12 Table of buffers for hBCAT extraction from IMR-32 cell lysate for activity assay. After the initial assay of buffers, buffer 2 was used as it maintained activity (Cooper *et al.* 2002; Faure *et al.* 1999; Suryawan *et al.* 1998; Thage *et al.* 2004; Torres *et al.* 1998).

Buffer	Contents
Buffer 1 – from Suryawan *et al*. (1998)	25 mM HEPES (pH 7.5); 0.4% CHAPS; 20 mM EDTA; 20 mM EGTA; 1x protease inhibitor; 5 mM DTT; 0.5 mM PLP
Buffer 2 – an altered version of that used by Suryawan *et al*. (1998)	25 mM HEPES (pH 7.5); 1% Triton X; 20 mM EDTA; 20 mM EGTA; 1x protease inhibitor; 5 mM DTT; 0.5 mM PLP
Buffer 3 – a combination of published buffers used for hBCAT	20 mM potassium phosphate (pH 7.5); 1 mM EDTA; 1 mM EGTA; 1x protease inhibitor, 20 mM DTT; 0.5 mM PLP
Buffer 4 – TCA buffer	20 mM Tris-HCl (pH 8.0); 50 mM ammonium acetate; 2 mM EDTA; 1x protease inhibitor; 20 mM DTT; 0.5 mM PLP

Abbreviations: HEPES - 4-(2-hydroxyethyl)-1-piperazineethanesulfonic acid; EDTA - ethylenediamine tetra-acetic acid; EGTA - ethylene glycol tetra acetic acid; DTT - dithioltheirtol; PLP - pyridoxal-phosphate .

polyclonal antibody raised to hBCATc 1/250 in blocking buffer, for cell only or secondary only controls – cells were re-suspended in blocking buffer only) and incubated on ice (30 minutes). The cells were centrifuged again, washed as previously described, and re-suspended in 200 µL of secondary antibody solution (Alexafluor 647 goat polyclonal antibody raised to rabbit IgG 1/250 in blocking buffer, for cell only controls – cells were re-suspended in blocking buffer only). These cells were incubated on ice in the dark (30 minutes), and subsequently and re-suspended in 250 µL of PBS and placed on ice until analysis (within 30 minutes). For determination of propidium iodide positivity, 2.5 µL was added to the PBS immediately prior to analysis on an accuri C6 flow cytometer. For all analysis, controls were analysed first and at least 10,000 live cells were counted.

4.6 Electron microscopy

4.6.1 Investigation of hBCAT and PDI subcellular localisation and co-localisation by Electron microscopy.

Cells were fixed by a 2x fixative solution (4% paraformaldehyde, 0.4% gluteraldehyde, 0.2 M phosphate buffer pH 7.4) in equal amount of complete medium (5 minutes, 37^{o}C). This was subsequently removed and replaced with 1x fixative solution (2% paraformaldehyde, 0.2% gluteraldehyde, 0.2 M phosphate buffer pH 7.4) (2 hours) prior to replacement with 1% paraformaldehyde fixative (1% PFA in 0.1M phosphate buffer) until sectioning. Embedding and sectioning were performed by University of Bristol staff according to the Tokuyasu method for cryosectioning (Slot & Gueze, 2007; Tokuyasu, 1973). Seventy nanometre sections were collected at -120^{o}C with 1% methylcellulose in 1.2 M sucrose and transferred onto copper mesh grids.

Copper grids were placed in PBS at 37^{o}C (30 minutes) prior to blocking with 100 mM glycine (10 minutes) and 0.1% acetylated BSA (10 minutes). Copper grids were placed in a primary antibody solution (Cambridge Biosciences rabbit polyclonal antibody raised to hPDI 1/10; Insight Biotechnology Ltd. rabbit polyclonal antibody raised to hBCATm 1/10) (1 hour) in advance of 0.1% acetylated BSA washes (3x5 minutes). Secondary antibody was again diluted in 0.1% acetylated BSA and applied (Aurion 6 nm gold conjugated secondary antibody raised to mouse IgG 1/20; Aurion 10 nm gold conjugated secondary antibody raised to rabbit IgG 1/20) (1 hour). The grids were washed as previously described and further washed in distilled water (3x5 minutes). The sections were counterstained with 0.3% uranylacetate in 1.8% methylcellulose on ice and imaged on a Technai 12 (FEI) transmission electron microscope at the University of Bristol.

4.7 Branched chain aminotransferase protein activity assay

4.7.1 Branched chain aminotransferase protein activity assay

The water bath was set at 37°C and the rubber caps and wells were prepared with filter paper. Wells containing filter papers had KOH (200 µL) added to absorb volatile carbon dioxide at the end of the experiment. Each experiment had a negative control (i.e. a sample lacking enzyme) and a positive control (i.e. a scintillation vial with 10 µL radioactive KIV added). To the glass vials 100 µL dH_2O, 100 µL $KiPO_4$, 20 µL 100 mM DTT, 50 µL KIV normal mix and 20 µL 5 mM PLP were added. The vials were added to the water bath in 20 second intervals. At 3 minutes 200 µL for cell homogenate was added to their appropriate vials (20 second intervals) and at 6 minutes, 500 µL of 3 M acetic acid (20 second intervals) was added to stop the reaction, and each vial was

capped. To each vial, 500 µL of H_2O_2 was added to convert remaining ketoisovalerate to carbon dioxide. The samples were subsequently allowed to remain at 37^{o}C for 60 minutes. Following this the caps were removed and the filter paper was discarded. Samples (150 µL) were added to each of the scintillation vials with 3 mL of scintillation fluid except for the positive control which had 10 µL of KIV added to 3 mL of scintillation fluid. The vials were vortexed in advance of measurement with the scintillation counter. This data was used to calculate BCAT activity.

4.8 Human branched chain aminotransferase protein over-expression and purification

4.8.1 Preparation of dialysis tubing

Dialysis tubing (14 kDa cut-off) was prepared by boiling in 1 L of dialysis tubing buffer (0.2 M $NaHCO_3$, 5 mM EDTA), washed in distilled water (3x) and repeated. The dialysis tubing was subsequently autoclaved in 500 mLs of distilled water and stored at 4^{o}C until use.

4.8.2 Human branched chain aminotransferase over-expression

2YT Luria-Bertani (LB) broth (1.6% Tryptone, 1% yeast, 0.5% NaCl) was autoclaved (120^{o}C, 20 minutes) and allowed to cool (1 hour) prior to the addition of kanamycin sulphate (to a final concentration of 12 µg/mL). To 250 mL of this kanamycin containing 2YT LB broth, *Escherichia coli* expressing the hBCATc or hBCATm gene (plus a kanamycin resistance gene) were added and incubated overnight (37^{o}C, 180 rpm). This was transferred to a 2 L culture of kanamycin containing 2YT LB broth and incubated again overnight (30^{o}C, 155 rpm). To induce hBCAT expression, 1 M IPTG was added (1 mL – 4 hours,

37^{o}C, 155 rpm) prior to centrifugation in a Beckman ultracentrifuge (4^{o}C, 12,000 x g, 5 minutes) to pellet the cells. This cell pellet was transferred to a 50 mL Corning tubes and stored at -80^{o}C overnight.

4.8.3 Human branched chain aminotransferase purification

Cell pellets were re-suspended in Buffer A (10 mM Tris, 0.1 M Na_2HPO_4, 1 µM β-mercaptoethanol, pH 8.0) for hBCATc or buffer AU (10 mM Tris, 0.1 M Na_2HPO_4, 5 M urea, 5 µM β-mercaptoethanol, pH 8.0) for hBCATm prior to sonication (15 second sonication intervals, with 10 second periods on ice). This was then centrifuged (12,000 x g, 10 minutes, 4^{o}C) and the supernatant removed. Ni-NTA-agarose (8 mL) was equilibrated and washed in buffer A or AU (3x) prior to having the BCAT supernatant (60 mL) added and mixed on a magnetic stirrer (4^{o}C, 1 hour). A Ni-NTA-agarose column was prepared and washed with buffers A (or AU) to D (buffer A – 10 mM Tris, 0.1 M Na_2HPO_4, 1 µM β-mercaptoethanol, pH 8.0; buffer AU – 10 mM Tris, 0.1 M Na_2HPO_4, 5 M urea, 5 µM β-mercaptoethanol, pH 8.0; buffer B – 10 mM Tris, 0.1 M Na_2HPO_4; 0.5 M NaCl, 5 µM β-mercaptoethanol, 20% glycerol, pH 7.4; buffer C – 10 mM Tris, 0.1 M Na_2PO_4, 1.5 M NaCl, 5 µM β-mercaptoethanol, 20% glycerol, pH 7.4; buffer C50 – 10 mM Tris, 0.1 M Na_2PO_4, 0.75 M NaCl, 5 µM β-mercaptoethanol, 75 mM Imidazole, 10% glycerol, pH 6.0; buffer D – 10 mM Tris, 0.1 M Na_2PO_4, 0.75 M NaCl, 5 µM β-mercaptoethanol, 750 mM Imidazole, 10% glycerol, pH 6.0) which eluted the hBCAT protein.

Nickel resin was eluted utilizing 1 mM EDTA and the G25 column was equilibrated in thrombin buffer (50 mM Tris, 150 mM NaCl, pH 7.5), the hBCAT proteins were exchanged into this thrombin buffer. Thrombin enzyme (100

units) was added to hBCAT proteins in thrombin buffer (30 mLs) (1 hour, 37^{o}C) prior to exchange into MonoQ buffer A (10 mM potassium phosphate buffer, pH 8.0) in the G25 column. The hBCAT protein in MonoQ buffer A was added to 3 mg of KIC in advance of further purification through a fast performance liquid chromatography machine (FPLC) utilizing a HiTrap Q ion exchange column. The FPLC was first equilibrated with MonoQ buffer A and MonoQ buffer B (10 mM potassium phosphate buffer, 0.5 M NaCl, pH 8.0) prior to the addition of the hBCAT protein. The hBCAT protein was eluted with increasing concentrations of salt into fractions of purity. These fractions were dialysed into stable buffer (50 mM Tris, 5 mM glucose, 1 mM EDTA, 1 mM KIC, 150 mM NaCl, 5 mM DTT, pH 7.5) by overnight (15 hour) incubation on a magnetic stirrer (4^{o}C). Fresh stable buffer was added and returned for a further hour. To this purified hBCAT, glycerol was added to 30% of the total volume and the protein was aliquoted (into 500 µL aliquots for activity assay, or 50 µL aliquots for Bradford protein concentration determination or Western blot controls) and frozen (-20^{o}C) until use.

5 Statistics

Throughout the results, where n numbers are appropriate, n^i refers to the number of individuals used in experimentation (e.g. an n^i of 80 on Western blot results means that 80 subjects underwent Western blot analysis) whereas n^e refers to the number of experimental repeats (e.g. an n^e of 15 on Western blot results means that 15 Western blots were performed in total, including repeats). Experiments were designed so that AD subjects (or cell treatments) were analysed alongside appropriate matched controls. For Western blot analysis, all gels included 4 AD subjects and 4 matched control subjects; for IHC, AD subjects were stained alongside matched control subjects; for cell culture, all treatments were performed and compared with untreated cells.

Densitometry data of hBCATc, hBCATm and glutathionylation was calculated by Image J software and taken to be normally distributed (parametric) interval data. Braak staging and small vessel disease score was considered ordinal data. Age, duration of AD, brain weight, post mortem delay, perineuronal net, parvalbumin positive neurons, insoluble amyloid, soluble amyloid, tau average (%) and frontal tissue pH were considered interval data. For the correlation of any density (hBCATc, hBCATm and glutathionylation) with either continuous or discrete variables (i.e. hBCATm vs. Braak stage, glutathionylation vs. age, etc.), Spearman's rho statistics was used. For comparison of density between two groups of individuals (i.e. AD vs control and male vs female), a two way ANOVA test was used. However, when comparing just a single set of groups (i.e. male vs. female) an unpaired t-

test was used. For comparison of density between more than two groups of individuals (i.e. APOE genotype, IRAP genotype, etc.), Kruskal-Wallis test was used. For comparison of staining scores between AD and control individuals, Wilcoxen-Mann-Whitney test was used. For cell culture work, where statistics were required, a student's paired t-test was performed.